NAT'L INST. OF STAND & TECH
A11106 484626
NIST
PUBLICATIONS
REFERENCE

National Bureau of Standards
Library, N.W. Bldg
APR 21 1964

Reference book not to be
taken from the library.

NBS

Technical Note 236

RESEARCH ON CRYSTAL GROWTH AND CHARACTERIZATION AT THE NATIONAL BUREAU OF STANDARDS JULY TO DECEMBER 1963

U. S. DEPARTMENT OF COMMERCE
NATIONAL BUREAU OF STANDARDS

NOV 14 1968
151670

NATIONAL BUREAU OF STANDARDS

Technical Note 236

ISSUED APRIL 6, 1964

RESEARCH ON CRYSTAL GROWTH AND CHARACTERIZATION AT THE NATIONAL BUREAU OF STANDARDS JULY TO DECEMBER 1963

Edited by H. Steffen Peiser
National Bureau of Standards

NBS Technical Notes are designed to supplement the Bureau's regular publications program. They provide a means for making available scientific data that are of transient or limited interest. Technical Notes may be listed or referred to in the open literature.

For sale by the Superintendent of Documents, U.S. Government Printing Office
Washington, D.C., 20402 - Price 40 cents

Contents

1. Introduction ---------- 1

2. Crystal Growth ---------- 2

2.1 Growth of Dislocation-Free Metal Crystals from the Melt ------- 2
2.2 Kinetics of Growth of Crystals from the Melt ---------- 4
2.3 Thermodynamics of Segregation of Solute Atoms to Stacking Faults in FCC Binary Alloys ---------- 6
2.4 Theory of Dendritic Crystallization ---------- 6
2.5 High-Temperature Crystal Growth ---------- 7
2.6 Study of Temperature Distribution in the Verneuil Process ----- 7
2.7 Crystal Growth and Structure Studies ---------- 7
2.8 Crystal Growth from Solution ---------- 8
2.9 Spherulitic Growth in Relatively Pure Systems ---------- 9
2.10 Homogeneous-Nucleation Studies ---------- 9
2.11 Single Crystals of Long-Chain Hydrocarbons ---------- 11
2.12 Crystallization of Polyethylene from the Melt ---------- 11
2.13 Theory of Crystallization of Bulk Linear Polymers ---------- 11
2.14 Crystallization of Polymers from Solution ---------- 12
2.15 Crystallization of Polyethylene Fractions ---------- 12
2.16 Electrodeposition of Single Crystals ---------- 14
2.17 Crystallographic Characterization of Pseudopentagonal Twins in Electrodeposited Copper Dendrites ---------- 14
2.18 Thermal Etching and Crystal Growth of Methane ---------- 14
2.19 Evaporation of Gold onto Cleaved Zinc Surfaces ---------- 16
2.20 Studies of Small Crystals of Nickel and Nickel Halides -------- 16
2.21 Kinetics of Whisker Evaporation ---------- 18
2.22 Theoretical Studies in Crystal-Whisker Growth ---------- 18
2.23 Growth Kinetics of Crystal Whiskers by Field-Emission Techniques ---------- 20
2.24 Field-Emission Studies of the Growth and Oxidation of Single Crystals ---------- 20
2.25 Condensation of Tungsten on a Cold Tungsten Substrate --------- 23

3. Defect Characterization ---------- 23

3.1 Magnetic Properties of Salt Single Crystals at Low Temperatures ---------- 23
3.2 Optical Properties of "Pure" and Impure Crystals, Paramagnetic Centers ---------- 24
3.3 Laser Microprobe for Analysis of Very Small Samples ---------- 24
3.4 Study of Crystal Defects ---------- 25
3.5 Defects in Thin Oxide Films ---------- 25
3.6 Effect of Point Defects on the Dynamic Properties of Crystals ---------- 27
3.7 Crystal Symmetry and Crystal Properties ---------- 27
3.8 Dislocations in Metals by Electron Microscopy ---------- 28
3.9 Growth of Helical Dislocations ---------- 28
3.10 Characterization of Electrodeposited Crystals ---------- 28
3.11 Second-Order Twinning in Aluminum ---------- 31
3.12 Accurate Measurement of Fundamental Electrical Properties of Semiconductor Crystals ---------- 31
3.13 Crystal Characterization of Diffraction Topography ---------- 33
3.14 Automation of Single-Crystal X-Ray Diffraction Intensity Measurements ---------- 37
3.15 X-Ray Studies ---------- 37
3.16 High-Voltage Laue Photographic Inspection of Large Single Crystals ---------- 37
3.17 Chemical Purity by Dielectric Cryometry ---------- 38
3.18 Optical Properties of Cadmium Sulfide and Telluride ---------- 38

3.19 Irradiation Studies ---------- 38
3.20 Development of Adiabatic Solution Calorimeter ---------- 38

4. Crystal Physical Properties ---------- 39

4.1 Reference Data on Single-Crystal Elastic Constants ---------- 39
4.2 Deformation and Fracture of Ionic Crystals ---------- 39
4.3 Studies in Solid-State Theory ---------- 39
4.4 Electronic Transport ---------- 40
4.5 Hall-Effect Measurements ---------- 40
4.6 Dielectric and Mechanical Properties ---------- 41
4.7 Dielectric Properties of Semiconductors ---------- 41
4.8 Crystals of Organic Molecules ---------- 43
4.9 Low-Temperature Thermometry ---------- 44
4.10 Oxide Melting-Point Standards ---------- 44
4.11 Dilatometric Studies of Polymers ---------- 44
4.12 Thermal Conductivity of Paramagnetic Crystals ---------- 45
4.13 Magnetic-Resonance Studies - I ---------- 45
4.14 Magnetic-Resonance Studies - II ---------- 46
4.15 Nuclear-Magnetic-Resonance Studies in Yttrium-Iron Garnets ---------- 48
4.16 Electron-Spin-Resonance Studies of Transition-Metal Complexes ---------- 48
4.17 Low-Temperature Nuclear Orientation ---------- 48
4.18 Microwave Measurements on Single-Crystal Ferrimagnetics ---------- 49
4.19 Adsorption on Metal Single Crystals ---------- 49
4.20 Superconductivity in Niobium ---------- 50
4.21 Experimental Determination of Atomic-Scattering Factors ---------- 50
4.22 Soft X-Ray Spectroscopy ---------- 50

5. Crystal Chemistry

5.1 Crystal-Structure Analysis ---------- 51
5.2 Crystal Chemistry of Calcium Phosphates ---------- 51
5.3 Standard X-Ray Diffraction Powder Patterns ---------- 52
5.4 Crystals with Large Lattice Spacings ---------- 52
5.5 Phase Equilibria ---------- 52
5.6 Allotropy in Some Rare-Earth Metals at High Pressures ---------- 53
5.7 Crystal Chemistry of Silver Iodide ---------- 53
5.8 Rapid X-Ray Diffraction Photography of Polycrystalline Materials ---------- 54
5.9 Structure of Silica Whiskers ---------- 54
5.10 Structure Models for Amorphous and Crystalline Phases of Simple Substances ---------- 55
5.11 Radial-Distribution Studies of Glasses ---------- 55
5.12 High-Resolution Small-Angle X-Ray Camera ---------- 55
5.13 Physical Structure of Crystalline Copolymers ---------- 56
5.14 High-Pressure Microscopy of Crystal Transformation and Growth ---------- 56
5.15 Optical Observations of Pressure-Induced Transformation in Polymers ---------- 57
5.16 Infrared Spectroscopy of Crystalline Inorganic Borates ---------- 57
5.17 Crystal-Field Studies by Matrix Spectroscopy ---------- 58
5.18 Spectroscopy of Diatomic Impurities in Rare-Gas Crystalline Matrices ---------- 58
5.19 Molecular Energy Levels ---------- 58

6. Partial List of Participants ---------- 59

7. Literature References ---------- 65

RESEARCH ON CRYSTAL GROWTH AND CHARACTERIZATION AT THE NATIONAL BUREAU OF STANDARDS JULY TO DECEMBER, 1963

Edited by

H. Steffen Peiser

Abstract

The National Bureau of Standards with partial support from the Advanced Research Projects Agency is continuing diverse research projects on the growth and characterization of crystals. This note summarizes the individual NBS activities in this and closely related fields during July to December, 1963. Lists of NBS publications appertaining to that period and of participating NBS scientists are appended.

1. INTRODUCTION

This is the third biannual collection of brief statements on research in progress at the National Bureau of Standards on crystal growth and characterization. In the first of these collections (NBS Technical Note 174, issued on March 15, 1963) the general purpose, background, and program area were described. They still apply, together with a few extensions that are explained in the second NBS Technical Note 197 (issued on September 23, 1963). The style, format, and principal headings adopted in the second biannual statment have been found convenient and have been used again in the research summary now presented for the period July to December, 1963.

Much of the work described is still being carried out with the support of the Advanced Research Projects Agency which, in anticipation of future technological demands in crystal science, is encouraging the National Bureau of Standards to produce pure and perfect reference crystals by newly developed techniques, if necessary, under closely controlled conditions, and to apply precise measurement techniques to the characterization of such crystals. The projects thus undertaken on behalf of ARPA are so closely interwoven with other projects carried on under the Bureau's own mission, that in a summary of the technical activities and results as is here presented, distinction cannot readily be made between the two kinds of projects. The ARPA initiative and support are therefore gratefully acknowledged here, but individual acknowledgements are not included in the text. Only in the few instances in which financial support from other agencies contributed to the program is an appropriate acknowledgement given.

Editorial work has been lightened by the efforts of Miss Lois L. Bardeen and the assistant editors who have represented the Bureau divisions as follows:

Electricity	I. L. Cooter
Metrology	P. E. Pontius
Heat	J. F. Schooley
Analytical Chemistry	L. J. Frolen
Mechanics	R. S. Marvin
Polymer	E. Passaglia

Metallurgy	R. L. Parker
Inorganic Solids	F. A. Mauer
Atomic Physics	H. P. R. Frederikse
Instrumentation	J. C. French
Physical Chemistry	D. E. Mann
Cryogenic Engineering	R. L. Powell
Radio Standards Physics	J. L. Dalke

The NBS "Crystal Group" has continued its lectures, visits, and informal colloquia. Contacts and collaboration with other research laboratories have been encouraging, and there have been several exchanges of special crystals. Harry C. Allen, Jr. is taking over the co-ordination of the NBS/ARPA program. In relinquishing his duties as co-ordinator, H. Steffen Peiser thanks all the contributors to this program. Much of its success depends on the quality and quantity of the research that still lies ahead, but the statements here presented may pave the way for significant contributions to crystal science.

2. CRYSTAL GROWTH

Contributions to this chapter are concerned with mechanisms and techniques of crystal growth and dissolution of single crystals.

2.1 Growth of Dislocation-Free Metal Crystals from the Melt

R. W. Dickson, Physical Properties Section,
H. C. Vacher, Metallurgy Division,
T. H. Orem, Corrosion Section, and
R. L. Parker, Crystallization of Metals Section

The background of this work is given in NBS Technical Notes 174, Section 4.3, and 197, Section 2.3. A major part of the effort on this project during the past six months has been spent in setting up the Lang camera on the Rigaku-Denki microfocus X-ray apparatus, and in learning techniques required for photographing dislocations with it. This camera, which is on loan from Rutgers University, was received in August, 1963, in lieu of the new unit to be delivered by Rigaku-Denki.

Prior to this time, the microfocus unit was employed in divergent-beam (pseudo-Kossel line) studies of single crystals of aluminum, bismuth, copper, germanium, lithium fluoride, calcite, and ammonium dihydrogen phosphate, ADP; 135 photographs of these crystals were taken. The method is found to give a good measure of lattice misorientations within a crystal down to about 3 minutes of arc. Although there is insufficient space here to summarize all the results, it should be mentioned that a number of Al crystals pulled by us from the melt, and several ADP crystals grown by Torgesen et al., Crystal Chemistry Section (compare Section 2.8) showed no discernible misorientation, within the above mentioned accuracy.

Since acquiring the Lang camera, we have taken about 160 photographs with it; these have been made on single crystals of Al, Si, Ge, and LiF. We first learned how to obtain good photographs of dislocations in Si. Due to space limitations, we present here only the results on Al crystals pulled from the melt of 99.999% purity. Figure 1 is a photograph of the crystal

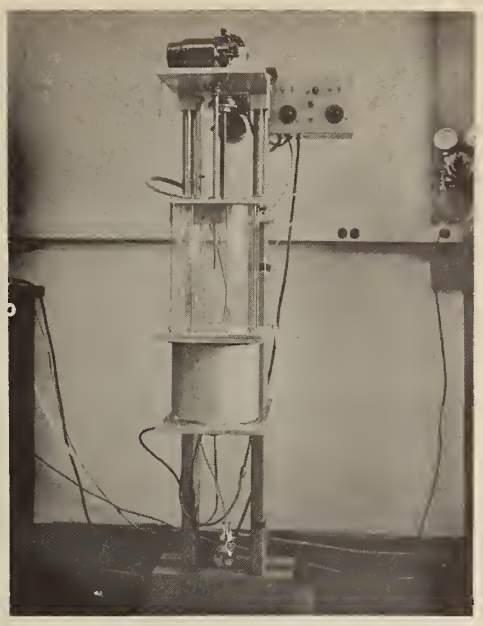

Fig.1 Crystal Puller

1cm

Fig.2 Optical photograph Al crystal #6

1mm

Fig.3 Dislocation topograph Al crystal #6

1mm

Fig.4 Al crystal #11

puller used in these experiments. Figure 2 is an optical photograph of one of the 12 Al crystals studied so far. It is here about 1.5 mm in diameter; it was etched down in aqua regia from its 4 mm original diameter. Figure 3 shows a dislocation topograph of a portion of this specimen. Particularly interesting are the small loops (~50 microns in size) which are seen, some of these having the form of two arcs of a circle. These loops are very similar in appearance to loops seen in quenched-aluminum foils by electron-diffraction contrast, although the latter are much smaller in size. It is possible that our loops are dislocation loops formed by collapse of vacancy disks which in turn are formed by the vacancy supersaturation occurring after cooling in the crystal puller. These loops have not been observed in thinner (~.1 mm) Al crystals (see Fig. 4). In this figure we do see regular bands of impurity build up near the tip; these correspond with thickening of the crystal at this point. Their regular separation of 0.86 mm coupled with the pulling speed of 0.33 mm/min gives a time spacing of 2.7 minutes, which corresponds with the cycle time of the temperature controller: as is known, impurity segregation occurs during temperature fluctuations. There is also a twisting effect, which is always of the same sense as the direction of crystal rotation, and which reverses when the rotation is reversed. Experiments are underway to eliminate this twisting effect, thought to be due to the torque exerted by an oxide skin on the melt surface. Al crystals grown at the Battelle Institute, Columbus, Ohio, under conditions similar to ours but without oxide skin on the melt have been received by us and are being examined.

In December, Dr. U. Bonse visited us and discussed his Cu-crystals work [Bonse et al., Physica Status Solidi, 3, K 355 (1963)] which shows that dislocation densities of $<500/cm^2$ can be obtained by pulling Cu crystals from the melt.

2.2 Kinetics of Growth of Crystals from the Melt

J. G. Early and R. L. Parker,

Crystallization of Metals Section

As outlined previously (see NBS Technical Notes 174, Section 4.4 and 197, Section 2.4) the objective of this project is to investigate the kinetics of the growth of crystals from the melt and, in particular, to study the role of interface temperature and orientation.

The experimental technique employed has been described theoretically by Tiller and Kramer [J. Chem. Phys., 37, 841 (1962)]. The technique permits the determination of the velocity of interface motion as a function of interface supercooling. Tiller and Kramer have successfully carried out several experiments on high-purity tin based on this method (as yet unpublished).

The first three months of this reporting period have been spent in accumulating the necessary equipment. Figures 5 and 6 are photographs showing the apparatus as used in several early experiments. A bell-jar type vacuum system has been purchased and installed which allows the experiments to be carried out at pressures in the range 10^{-6} to 10^{-7} torr. A motor-driven Variac provides a periodically varying current to the heater that floats on top of the liquid metal in the crucible. The heater establishes a periodic temperature wave within the metal in the crucible. A fixture has been assembled to fit inside the bell-jar to hold the crucible, measuring thermocouples, and the heater. Amplifying and recording equipment have been set up to provide the necessary instrumentation.

Periodic temperature waves (having an amplitude of less than 0.001°C with a period of 30 seconds) have been generated, measured, and recorded. Several preliminary experiments have been performed with the apparatus on 99.9% pure tin. This was done to check out the operation of the various

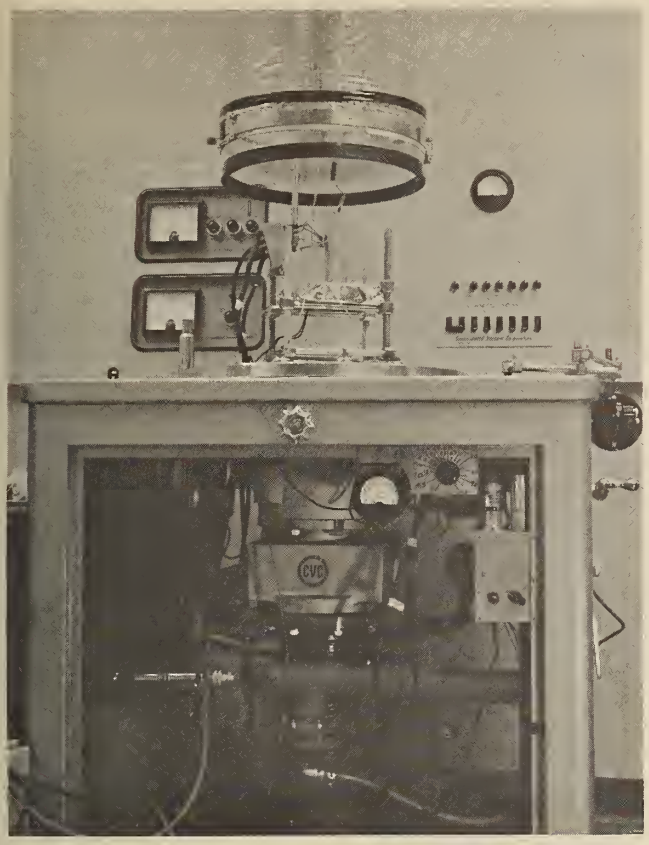

Fig.5 Photograph of apparatus showing vacuum system with bell-jar in raised position, motor-driven Variac as used in growth studies

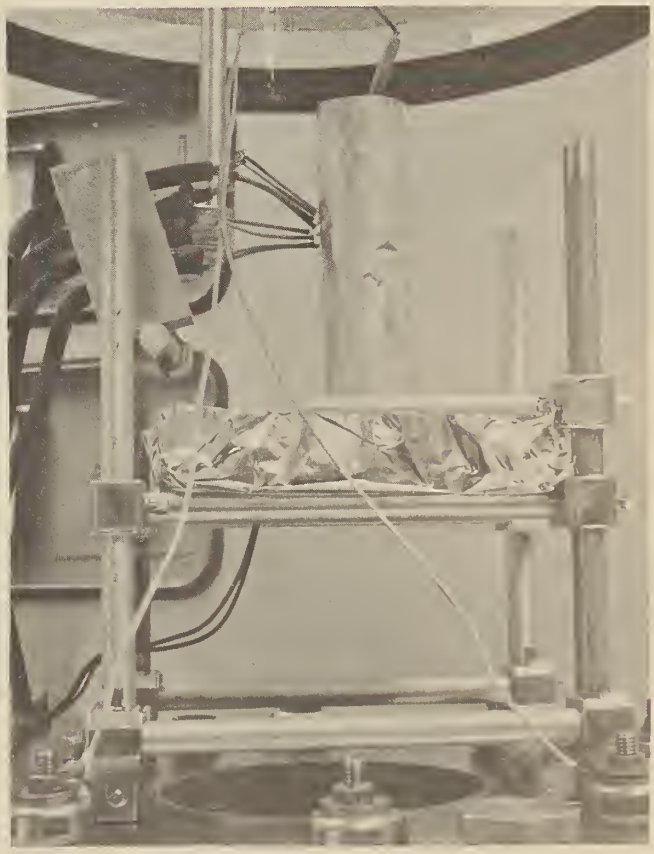

Fig.6 Close-up showing crucible with an aluminum radiation shield, thermocouples and heater mounted on vacuum-system base plate

components of the apparatus and to observe the effect on a thermocouple signal of the passage of the solid-liquid interface past the thermocouple. An attempt was also made to determine the position of the solid-liquid interface under equilibrium conditions.

Additional experiments are now in progress on single-crystal samples of 99.999 and 99.9999% tin. Later, experiments will be made on lead of 99.999 and 99.9999% purity. At present, a number of seed single crystals of 99.999% tin have been grown by an inverted Bridgman technique. These seeds will be used to grow large single crystals in the measuring crucibles.

2.3 Thermodynamics of Segregation of Solute Atoms to Stacking Faults in FCC Binary Alloys

R. deWit,

Lattice Defects and Microstructures Section, and

R. E. Howard,

Metal Physics Section

Instead of assuming with others [Dorn, Acta Met., 11, 218 (1963), and Suzuki, J. Phys. Soc. Japan, 17, 322 (1962)] that the width of the extended dislocation remains fixed during segregation, we suppose that the width always has the equilibrium value corresponding to the local concentration at the fault and thus changes continually. The condition for thermodynamic equilibrium between the fault and the bulk becomes

$$\Delta\mu_A - \Delta\mu_B - (V/t)(d\gamma/dc^f) = -(d\gamma/dc^f)[(1-c)\Delta\mu_A + c\Delta\mu_B]/\gamma$$

which differs from the previous work, referred to above, where the right hand side was equated to zero. Here A and B denote solvent and solute atoms, respectively, f the faulted region of thickness t, $\Delta\mu = \mu^f - \mu$ is the difference in chemical potential between the faulted and unfaulted regions, c the concentration of solute atoms, γ the stacking fault energy, and V the molar volume. A consequence is that, unless a miscibility gap exists, $\gamma>0$ for all concentrations. Hence, contrary to Suzuki, the stacking fault width can never increase indefinitely. If the γ-c curve is known for the unsegregated alloy, we can find the γ-c curve for the fully segregated alloy by numerical solution of our equation. The latter curve always lies below the former. If the latter curve describes the results of node-analysis experiments and the former those of work-hardening experiments to measure the stacking-fault energy, then our theory resolves some of the discrepancy that exists in the literature [Thornton, Mitchell, and Hirsch, Phil. Mag., 7, 1349 (1962)].

2.4 Theory of Dendritic Crystallization

S. R. Coriell and R. L. Parker,

Crystallization of Metals Section

This project was started on December 18, 1963. Preliminary plans are to study diffusion-controlled growth of crystals, with particular emphasis on the conditions necessary for dendritic growth to occur. Our problem of interest is the solution of the diffusion equation with a time-dependent boundary condition. Previous work in this area is being studied. Of particular importance is a recent article by Mullins and Sekerka [J. Appl. Phys., 34, 323 (1963)] in which the stability of the shape of a spherical particle undergoing diffusion-controlled growth is considered. They show that the sphere is stable below and unstable above a certain radius. Further work along these lines appears to be desirable. As a start, the cylindrical symmetry problem is being worked through.

2.5 High-Temperature Crystal Growth*

W. S. Brower and E. N. Farabaugh,
Crystal Chemistry Section

Work described earlier (NBS Technical Notes 174, Section 4.1, and 197, Section 2.1) has been continued with the purpose of determining the influence of growth parameters on the perfection of refractory-oxide crystals.

Crystals of rutile grown at widely varying rates (0.3-12 cm/hr) were examined by an etch technique in an effort to determine the effect of growth rate on crystal perfection (compare Section 2.7). It was found that the dislocation densities ($\sim 5 \times 10^6 cm^{-2}$) did not vary significantly from the slowest to the most rapidly grown crystal. The examination of the series of samples is being continued to determine if there is any significant variation in the number and size of the sub-grains.

The high-frequency (45 - 90Mc) rf induction heater has been put into operation and various coil designs have been investigated to obtain the optimum configuration for direct coupling. Slightly reduced rutile has been successfully melted, with the improved coil designs. The present aim is to use either rutile or another oxide having a rather high electrical conductivity near its melting point in initial attempts at floating-zone crystal growth of semiconductor materials.

2.6 Study of Temperature Distribution in the Verneuil Process*

F. Ordway,
Inorganic Solids Division, and

P. R. Miller,
Crystal Chemistry Section

Measurements of temperature in the growing crystal during the flame-fusion process have been made with Ir/60% Ir-40% Rh thermocouples. The measurements indicate that a very high vertical temperature gradient exists in the portion of the boule near the cap, and this decreases proportionally with the logarithm of the axial distance to a constant gradient that is very small by comparison. Existing theories agree with the results only in a rough qualitative manner. The theoretical problem is being studied further, and attempts are being made to determine the radial temperature gradients.

2.7 Crystal Growth and Structure Studies

D. E. Roberts,
Solid State Physics Section

Cadmium telluride, CdTe, is being prepared by the Bridgman technique as described in the previous report. CdTe is now also obtained by vapor growth in a closed tube at temperatures from 800°C to above 1000°C. The resulting crystals have the form of needles, platelets, or cubes of a few millimeters in dimension.

---

* This work was partially supported by the Atomic Energy Commission.

Crystals of cadmium sulfide, CdS, have been prepared from the vapor phase. Growth occurs at temperatures from 900-1100°C in a vacuum or in an atmosphere of hydrogen sulfide, H_2S. Crystals are in the form of needles or platelets of a few millimeters in dimension. The virgin surfaces of vapor-grown materials are especially valuable for optical measurements.

Rutile, TiO_2, is being grown by the Verneuil technique. The present emphasis is on the preparation of boules of a larger size and a higher degree of perfection (compare Sections 2.5 and 3.15).

A number of attempts have been made to diffuse impurities into samples at high temperatures. Samples include TiO_2, strontium titantate, $SrTiO_3$, magnesium fluoride, MgF_2, and lead fluoride, PbF_2. Success has been very limited, but further attempts will be made.

2.8 Crystal Growth from Solution

J. L. Torgesen, A. T. Horton, and J. Strassburger,
Crystal Chemistry Section

Single-crystal growth from aqueous solution by temperature-program techniques (see NBS Technical Notes 174, Section 4.5, and 197, Section 2.5) has continued to produce specimens of ammonium dihydrogen phosphate (ADP) (pure, and containing chromium impurity) and sodium chlorate (pure, and containing copper impurity). Crystals of ADP, growing in the presence of chromic ions, show the tapered habit and retention of chromium adjacent to the tapered vicinal faces. They revert essentially to normal habit on continued growth after the chromic ion activity is reduced to a low value by the addition of a complexing agent, ethylenediamine tetraacetic acid.

Habit changes in sodium chlorate single crystals grown in the presence of cupric ions are characterized by greater predominance of {110} and {111} faces. Spectrographic analysis of sectioned portions of the crystals indicates cupric-ion content in material deposited on the growth surfaces differing for the various faces in the order {111}>{100}>{110}.

Limited success has been achieved in the growth of potassium and sodium chloride from pure aqueous solution. Crystal faces are rough and polycrystalline growth is common. Experiments on the effect of pH in the growth of small seed crystals of sodium chloride indicate that pH range 3 to 5 yields seed crystals of better quality than those grown in more acid or neutral solutions. Moreover, the danger of OH^- ion contamination would be expected to be reduced at lower pH.

An effort to produce (KAP) potassium acid phthalate single crystals of adequate size and perfection for long-wavelength X-ray spectroscopy is presently being initiated (see Section 3.13 of this Technical Note). The crystals will be grown both by a temperature-programming technique and by an isothermal solvent-evaporation method [Karpenko et al., Sov. Phys. Cryst., 6, 120 (1961)].

Characterization of ADP crystals by X-ray diffraction topography (see Section 2.1, and especially 3.13) has shown the specimens to be of high intrinsic quality. Particularly important in these investigations have been the methods of surface preparation. It has been shown, as was suspected from earlier work on other materials, that conventional techniques of abrasive-wheel cutting, followed by grinding and polishing, introduce many dislocations. Sectioning of the crystals with a string-saw, using water as the solvent, followed by etch-polishing with ethyl alcohol-water mixtures, produces specimens in which high intrinsic perfection is retained. Relatively large areas of the specimens are essentially dislocation free and show strains only of long-range order. Flat etch-polishing is accomplished by rotating

and advancing the crystal specimen closely adjacent to, but not touching, a rotating glass plate over which flows a thin film of the alcohol-water etchant.

The growth of single crystals of sparingly soluble salts in silica gel has continued to be used in the production of a variety of materials. Of special note are crystals of calcium tartrate (up to 1 cm in longest dimension) possessing well-developed habit and good optical quality, and calcium carbonate (up to 1 mm in diameter). Phase changes in the mercuric iodide system have been observed visually and by time-lapse photography through the microscope. The change from the first-formed yellow mercuric iodide to the red form is not a solid-solid transition, but follows a dissolution and regrowth mechanism. However, if the surrounding silica gel is allowed to dry, a solid-solid transition from the red to the yellow form ensues.

In the lead-iodide system the crystallization of the mono- or di-iodide is dependent on localized iodide-ion concentration. First-formed di-iodide changes to the mono-iodide with reduction of iodide concentration by diffusion. The formation of dendritic metallic copper in tetrahedra by reduction of the cupric ion results from the crystallization of an intermediate oxide of copper (possibly Cu_4O) in tetrahedral habit, with retention of this habit as reduction to the metal proceeds. The silica-gel method for growing single crystals seems most applicable to materials having solubilities of the order of hundredths of one percent. Little success has been achieved to date with very slightly soluble salts such as the silver halides and metallic sulfides.

2.9 Spherulitic Growth in Relatively Pure Systems

G. S. Ross and L. J. Frolen,
Analytical Chemistry Division

In some conditions in many materials, the observed mode of crystal growth is spherulitic. In general, spherulite-forming systems have a high impurity content, and the spherulites have a small radial growth rate. Keith and Padden [J. Appl. Phys., 34, 2409 (1963)] proposed a phenomenological theory explaining spherulitic growth in both polymer systems and others which are characterized by their high impurity content.

Recently it was observed that diphenylalkanes form spherulites, but in contrast to the Keith-Padden systems, these materials have a low impurity content and the radial growth rate is very rapid. In both types of systems, material is deposited between the spherulitic fibers. In the Keith-Padden systems, this material is assumed to be impurity and it may or may not crystallize after the initial spherulitic growth. In our systems, the interfibrillar material must be nearly pure diphenylalkane. We postulate that this material exists in a glassy state during the spherulitic growth but that it in turn crystallizes as the sample is warmed. Crystallization is observed after the original spherulitic formation as shown in the series of pictures (Fig. 7, a-d). Work on the spherulite-forming diphenylalkanes is being continued. The results obtained are inconsistent with the Keith-Padden theory, and we feel the theory must be modified if it is to include spherulitic growth in nearly pure systems.

2.10 Homogeneous-Nucleation Studies

F. Gornick,
Polymers Division, and
G. S. Ross, L. J. Frolen, and D. J. Termini,
Analytical Chemistry Division

Characterization of a group of well purified diphenylalkanes has been

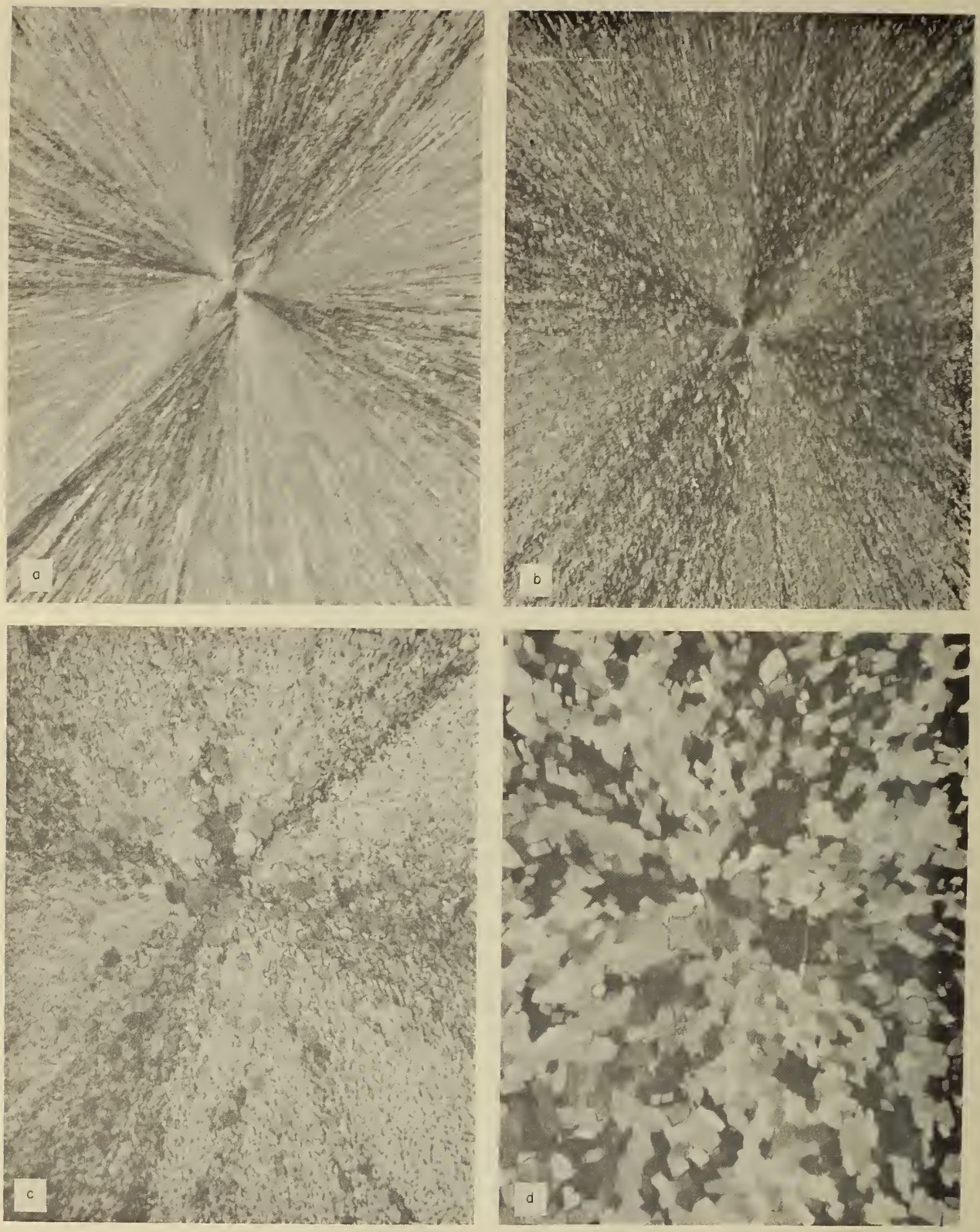

Fig. 7 Spherulites of 1,2-diphenylethane, showing crystallization phenomenon which occurs at room temperature. (a) Spherulite formed in alcohol bath, cooled to -75°C; (b) after 1/2 min atm. T (c) after 1 min atm. T (d) after 6 min atm. T

continued (see NBS Technical Note 197, Section 2.8). Dilatometric studies of several members of the series are being completed to establish the existence of solid-solid phase transitions. The viscosities of 1,4-diphenylbutane and 2,2-diphenylbutane have been measured over a 100-degree temperature range including the supercooled liquid region.

A cinephotomicrographic assembly for both time-lapse and variable continuous speed-photography has been ordered and will be received and tested in January. Development of apparatus and techniques for the study of homogeneous nucleation in both polymeric and non-polymeric systems is being continued.

2.11 Single Crystals of Long-Chain Hydrocarbons

J. M. Crissman and E. Passaglia,

Polymers Physics Section

An attempt is being made to grow large single crystals of the n-alkanes $C_{32}H_{66}$ and $C_{94}H_{190}$. These crystals, which are model systems for polymer crystals, are to be used to determine various physical properties of these materials, in particular, the elastic constants.

The method used is the modification of the Bridgman technique developed by Horton [U. S. Patent No. 2754180, issued July 10, 1956]. So far only polycrystalline aggregates of both materials have been produced, and it is speculated that this is caused by insufficient purity of the starting compounds.

In $C_{94}H_{190}$, which has been examined in some detail, the crystals grow such that the [010] direction is along the temperature gradient. This is undesirable, since this is the fastest growing direction. Means of inducing the crystal to grow with [001], the slowest growth direction, along the temperature gradient are being tried.

2.12 Crystallization of Polyethylene from the Melt

J. J. Weeks,

Dielectrics Section

In a previous publication [Weeks, 1963] the observed increase in the melting temperature of linear polyethylene with increase of crystallization time was interpreted to be a result of isothermal thickening of the lamellae. Direct experimental verification of the thickening by low-angle X-ray diffraction measurements is desirable in assessing the possible importance of increased crystal perfection as an explanation for the melting behavior. Since measurements will have to be made at the crystallization temperature, a hot stage is required. This stage has been constructed and its control characteristics are being determined.

2.13 Theory of Crystallization of Bulk Linear Polymers

J. D. Hoffman,

Polymers Division

A review article, "Theoretical Aspects of Polymer Crystallization with Chain Folds: Bulk Polymers", has been prepared for publication. The theory of crystallization of bulk linear polymers with chain folding is discussed in terms of recent developments. Specific topics covered are: (a) rate of crystal growth and size of folded nuclei; (b) theoretical and experimental

estimates of the fold-surface free energy, and estimates of the surface free energy of "fringed micelle" and "switch-board" type crystals; (c) basic causes of essentially regular folding in bulk; (d) rejection of short-chain species during crystallization; (e) melting behavior of thin chain-folded lamellae; (f) gradual thickening of lamellae on isothermal storage; (g) homogeneous, pseudohomogeneous, and heterogeneous nucleation; (h) voids and included point defects as a part of the concept of the degree of crystallinity; and (i) phenomena occurring in Stage 1 and Stage 2 of bulk crystallization isotherms (annealing). A comparison of theory and experiment is carried out by means of data, some previously unpublished, on polyethylene and polychlorotrifluoroethylene. The theory with essentially regular folding is found to be satisfactory.

2.14 Crystallization of Polymers from Solution

F. Khoury,

Polymer Physics Section

Polypropylene crystallizes isothermally at 110 - 115°C from $\frac{3}{4}$% solutions in amyl acetate in the form of aggregates which exhibit an apparent polyhedral habit under the optical microscope. These aggregates, which are square or slightly rectangular-shaped, of approximately uniform size (sides 4-5μ) and overall thickness (~2μ) possess a composite (distinct from single-crystal) morphology, features of which are specifically related to their habit. Replicas of their largest surfaces (parallel to the square cross-section) reveal (under the elecrron microscope) an open network consisting, apparently, of two sets of narrow (~200 Å) ribbon-like fibrils oriented with their respective lateral edges at ~90° to one another and at ~45° to the sides of the square (or rectangular) shaped periphery (Fig. 8). A narrow fringe of similarly oriented intercrossing fibrils is detected in transmission around the latter periphery; the aggregates are otherwise essentially opaque to the electron beam (Fig. 9). Distinctly lamellar structures have also been observed in the peripheral regions of some aggregates. The lattice orientation in the fibrils and lamellae as well as the origin of the dual morphology and pseudopolyhedral habit of these aggregates, samples of which exhibit a monoclinic [Natta et al., Atti accad. nazl. Lincei Rend., Classe Sci. Fis. Mat. e Nat., 21, 363 (1956)] X-ray powder diagram are being investigated. The elucidation of these features should provide information pertinent to a better understanding of the mechanism of crystallization of polypropylene in general and spherulitic crystallization in particular, since structures exhibiting a similar habit to that described above have been observed (under the optical microscope) to form during the early stages of development of polypropylene spherulites.

2.15 Crystallization of Polyethylene Fractions

R. C. Neuman and J. Powers,

Macromolecules: Synthesis and Structure Section

The thermal conditions for which linear polyethylene shows a morphological change (from a ringed spherulite to a granulated crystal habit) have been reported previously (NBS Technical Note 197, Section 2.7). Increases in low-angle X-ray diffraction spacing, partial melting and recrystallization, and increases in lamellar thickness have already been reported in the literature for these same thermal conditions. We are testing our postulate, therefore, that the common crystallization mode in polymers (spherulitic nucleation and then growth) is complicated by the existence of lamellar-thickness changes in the temperature range in which polyethylene spherulites might be expected to develop slowly.

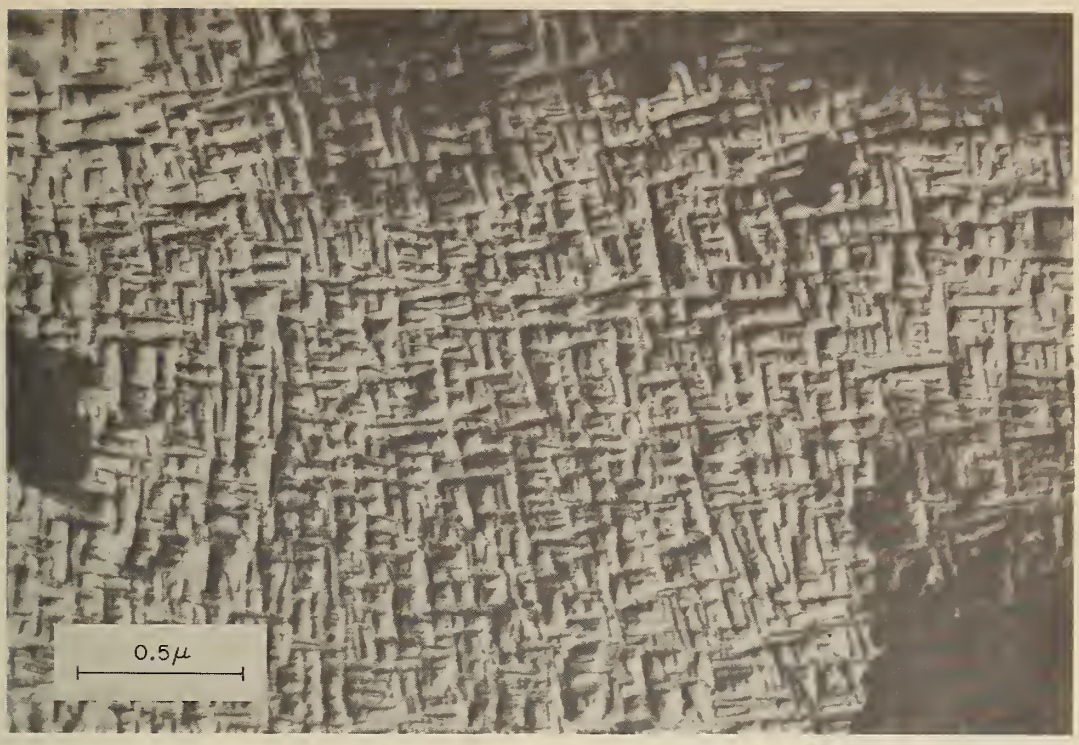

Fig.8 Carbon replica of the surface of a pseudopolyhedral aggregate of polypropylene revealing an apparently intermeshed fibrillar structure. The sides of the aggregate with respect to this electron micrograph coincide in orientation with those of the aggregate shown in Fig. 9.

Fig.9 Transmission electron micrograph of a polypropylene aggregate exhibiting its pseudopolyhedral habit and fringe-like peripheral morphology.

2.16 Electrodeposition of Single Crystals

F. Ogburn and J. D. Young,

Electrolysis and Metal Deposition Section

Under suitable conditions copper will grow epitaxially when electrodeposited on a copper single crystal. This seemed to offer a promising method of growing large single crystals of copper by electrodeposition with a seed crystal to initiate the process. Initial attempts, however, led to polycrystalline deposits except for the first microns of deposit (Ogburn and Newton, 1963). Efforts are being continued to develop this technique for growing massive single-crystal deposits of copper. Some progress has been made in that single-crystal deposits about 10 mm x 10 mm x 2 mm now have been obtained, but not without polycrystalline material on the sides.

2.17 Crystallographic Characterization of Pseudopentagonal Twins in Electrodeposited Copper Dendrites

B. Paretzkin and H. S. Peiser,

Crystal Chemistry Section, and

F. Ogburn,

Electrolysis and Metal Deposition Section

A brief note has been written on the pseudopentagonal twins reported in NBS Technical Note 197, Section 2.10 (Ogburn, Paretzkin, and Peiser, 1964).

The unusual crystallographic twinning is possible because of the ⟨110⟩ elongation coupled with the angle $111\widehat{\ }1\bar{1}1$ being 70°32' or nearly 360°/5. Since there is a twofold axis of symmetry parallel to [110] most features of the twin can be described equally well in terms of pseudodecagonal symmetry. Figure 10 shows the angular relationships in the [$1\bar{1}0$] zone for the {111} faces of a crystal A that is twinned by rotation about [111] producing crystal B and about [$11\bar{1}$] producing crystal C. Further twinning of B about its [$11\bar{1}$] and C about its [111] introduces only two new crystals having orientations D and E, respectively. The planes ($\underline{\underline{111}}$) of D and ($\underline{\underline{11\bar{1}}}$) of E [just as ($\underline{111}$) indicates the position of (111) after twin operation, so ($\underline{\underline{111}}$) here indicates the position of (111) after two twin operations, the first of which left it unchanged] are inclined by 7°20' to each other, this being five times the difference between 360°/5 = 72° and the above mentioned angle $111\widehat{\ }11\bar{1}$ = 70°32'. Theoretically only three individuals are needed to show full pseudodecagonal (or pseudopentagonal) character; A, B, and E; or A, B, and D; but in practice orientation E can be achieved only through orientation C, and D only through B; so a minimum of four individuals are really needed for this pseudosymmetry. It is easily seen how, by repeated twinning, pairs of {111} faces at 7°20' to each other can be introduced all around the zone. A considerable number of repetitions can produce a twin displaying clear pseudopentagonal character; but as the number of twin operations becomes large, angles that are multiples of 7°20' will appear until eventually the twin may resemble a polycrystalline sample with ⟨110⟩ fiber orientation.

2.18 Thermal Etching and Crystal Growth of Methane

G. L. Pollack and R. S. Willams,

Crystal Chemistry Section

The techniques which were previously developed for growing and etching rare-gas solids are being extended to other molecular crystals and, in particular, have already been used to grow crystals of methane of about

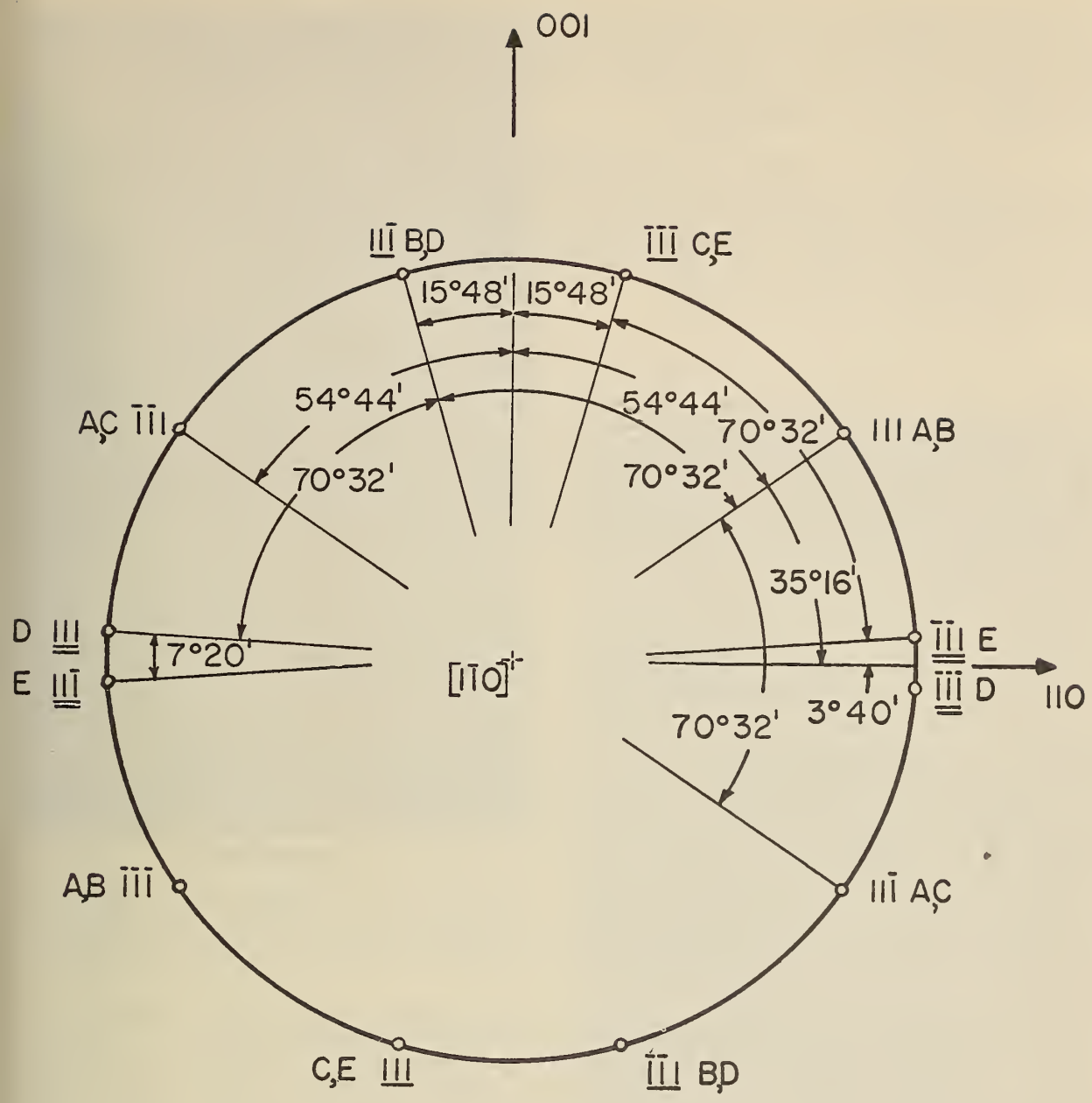

Fig.10 Angular relationships of {111} faces in [110] zone of cubic crystals twinned repeatedly to produce pseudopentagonal symmetry along the zone axis.

A indicates original crystal.
B indicates crystal obtained by twinning A by [111] rotation.
C " " " " " A " [11$\bar{1}$] "
D " " " " " B " [$\underline{11\bar{1}}$] "
E " " " " " C " [$\underline{111}$] "

centimeter dimensions in a polycrystalline block (Williams and Pollack, 1964). The crystals are thermally etched so that single grains and growth habits may be visually observed. These habits have been studied as functions of crystal growth rate (0.5 cm/hr - 5 cm/hr), impurity content, initial nucleation conditions, and other parameters.

The research is aimed at accomplishing two things, the first of which is the preparation of large crystals suitable for study of the low-temperature solid-state properties of methane. Ultrasonic-velocity and elastic-constant determinations as well as thermal-conductivity and diffusion measurements can be undertaken most meaningfully on large single crystals. Crystals have already been grown of sufficiently good quality and size so that measurements of this kind are practical.

The second aim is to study the mechanism of solid-solid phase nucleation. Methane is the simplest molecular solid with a phase change suitable for such a study and it is proposed to observe crystal growth and crystal properties in the region of the change which occurs at about 20°K. Thus far, observations on suitable crystals have extended from the triple-point temperature (about 89°K) down to 77°K, and the experiments are shortly to be extended to even lower temperatures. The grain sizes are apparently rather little changed by these variations in temperature and no unconquerable difficulties in reaching 20°K and below are as yet anticipated.

2.19 Evaporation of Gold onto Cleaved Zinc Surfaces

L. K. Ives and A. W. Ruff, Jr.,

Lattice Defects and Microstructures Section

The initial stages of nucleation and growth of gold vacuum deposited on freshly cleaved {0001} zinc surfaces have been studied by replica electron microscopy. To assist in interpretation, cleaved rock-salt surfaces were placed adjacent to each zinc sample prior to evaporation. Evaporation rates were typically one monolayer/minute in an ambient vacuum of 10^{-5} torr. The average gold thickness was varied from about one to ten monolayers.

The results on as-cleaved rock-salt surfaces were in agreement with those of Bassett. Isolated gold nuclei (diameter 20-50 Å) were found at all coverages. Cleavage steps were visibly decorated down to monatomic heights (Fig. 11).

As-cleaved zinc surfaces also exhibited isolated gold nuclei, less regular in shape than those on the companion rock-salt surface (Fig. 11). Long linear chains of nuclei were observed and interpreted to indicate surface steps. These decorated steps occurred much less frequently than on rock salt. A series of zinc samples were deformed and a small fraction of the slip steps produced showed preferential gold nucleation. It is believed that impurity contamination of the zinc surfaces strongly affects the nucleation and growth processes in comparison with the rock-salt results. Current efforts involve a study of different replication methods and their effect on the observed distribution of nuclei.

2.20 Studies of Small Crystals of Nickel and Nickel Halides

D. R. Winder,

Radio and Microwave Materials Section

Nickel whiskers, nickel halide whiskers, and platelets have been grown for studies of dimensionality in magnetism. The conditions for growth of these crystals have been studied and the growth characteristics of the

a

b

Fig. 11 Carbon extraction replicas of deposited gold film, average thickness about 3 monolayers; (a) as-cleaved rock-salt substrate illustrating gold nuclei and step decoration; (b) as-cleaved zinc substrate illustrating some step decoration and clustering of nuclei.

platelet habit investigated. A paper by Winder and Sickafus on the last subject was presented at the Pasadena Meeting of the American Physical Society in December, 1963. The abstract follows:

"Crystals of $NiBr_2$ and $NiCl_2$, grown by sublimation, exhibit dendrites and platelets having circular growth spirals, trigonal symmetry, and deliquescent properties. Fizeau interferograms are utilized to determine step heights of the spirals. Growth spirals on opposite sides of a platelet are shown to be related. Appearance of isolated concentric spirals, not only of the expected opposite sense but also of the same sense, and of large step height indicate that large variations in Burgers vectors occur through the connecting region. Trigonal symmetry is displayed by the dendritic structure and polygonal growth structure."

2.21 Kinetics of Whisker Evaporation

R. L. Parker, S. C. Hardy, R. L. Anderson, and
T. Wagner,
Crystallization of Metals Section

On this project, the reader should refer to NBS Technical Notes 174, Section 4.16, and 197, Section 2.15. A paper entitled, "Growth and Evaporation Kinetics and Surface Diffusion of K and Hg Crystal Whiskers", (Parker, Anderson, and Hardy, 1963) has been published during this reporting period. We have continued our study particularly on the growth and evaporation of Hg whiskers, and have obtained about 700 photographs taken under different conditions of super-saturation and temperature.

Figure 12 shows a typical growth and evaporation sequence for Hg. There is some evidence that $\log\lambda$ is a linear function of $1/T$, T being the absolute whisker temperature, but the data have considerable scatter. The phenomenon of snapping or tipping noted earlier for K whiskers [Anderson and Parker, Bull. Am. Phys. Soc., 8, 393 (1963)] has been observed and studied in Hg whiskers. Both abrupt and gradual rotations of the whisker about its point of attachment to the substrate can be observed; these angles varied from 0 to 90°, in as many as 50% of the whisker population. A complete reversal to the original position often occurs. The motion, not to be confused with Brownian motion which is also observed, can sometimes be induced by vibration. The mechanism of this effect is not known.

A study of the causes underlying stoppage of length growth in Hg whiskers was begun. It is proposed to use our present data on this to compare and evaluate the four current theories relating to this effect.

2.22 Theoretical Studies in Crystal-Whisker Growth

J. A. Simmons and R. E. Howard,
Metal Physics Section,
R. L. Parker,
Crystallization of Metals Section, and
H. J. Oser,
Computation Section

In NBS Technical Note 197, Section 2.16, the background to this work is described. The implicit solution for the time-dependent whisker-growth problems has been extended to include the more realistic assumption that the surface concentration at the tip remains at the equilibrium concentration with the surrounding vapor.

GROWTH

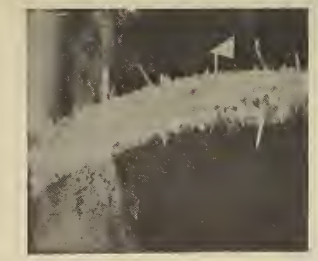

59 min.

61 min.

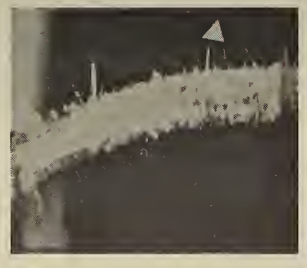

65 min.

72 min.

T_o = -68°C, P_o = 2.48 x 10^{-5} μ Hg

T = -40°C, P = 2.18 x 10^{-3} μ Hg

500 μ

EVAPORATION

90 min.

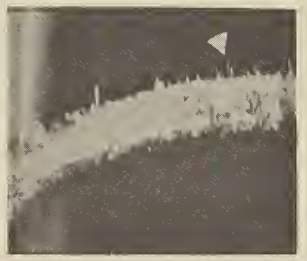

109 min.

137 min.

244 min.

T_o = -68°C, P_o = 2.48 x 10^{-5} μ Hg

T = -76°C, P = 5.2 x 10^{-6} μ Hg

α = P/P_o = 0.210

Fig. 12 Growth and evaporation of mercury whiskers from the vapor phase

Although the explicit numerical computation for x(t) is not yet available, due in part to programming difficulties, the following asymptotic results have been established:

$$\dot{x}(t) = \gamma \sqrt{\frac{D\mathcal{J}}{1+\gamma\mathcal{J}}} \text{ when either } x(t) \gg \sqrt{D\mathcal{J}} \text{ or } x(t) \gg \sqrt{\frac{D}{\gamma}}$$

and

$$\dot{x}(t) = \gamma\, x(t) \text{ when } x(t) \ll \text{both } \sqrt{D\mathcal{J}} \text{ and } \sqrt{\frac{D}{\gamma}}\ .$$

Here γ is the growth constant, D is the coefficient of surface diffusion, $\mathcal{J}$ the mean time for an atom on this whisker surface to evaporate, and x(t) is the position of the whisker tip at time t as measured from the substrate.

From this expression for the limiting linear velocity it is found that the approximate quasi-steady-state solutions derived by Blakely and Jackson [J. Chem. Phys., 37, 428 (1962)] and Dittmar and Neumann [Z. Elektrochem., 64, 297 (1960)] are correct only in the limit $\gamma\,\mathcal{J} \ll 1$. When $\gamma\,\mathcal{J} \gg 1$, the discussion of whicker-growth rates by Gomer [J. Chem. Phys., 38, 273 (1963)] seems qualitatively correct.

The equations and limiting linear velocity for growth have also been found to be valid for the case of whisker evaporation. Further publications are pending (Simmons, Parker, and Howard, 1964; and Simmons, Howard, and Parker, 1964).

2.23 Growth Kinetics of Crystal Whiskers by Field-Emission Techniques

S. C. Hardy and R. L. Parker,

Crystallization of Metals Section

Well developed, symmetric patterns have now been obtained from potassium whiskers grown from the vapor at a much greater pressure than had been used previously. This was done by heating a potassium-coated wall opposite the substrate; allowing the tube to cool in order to reduce the vapor pressure; and then examining the emission patterns. Figure 13 shows a field-emission pattern from a [100] oriented whisker. [110] oriented patterns were also photographed. Patterns of uniform emission are often seen simultaneously with symmetric patterns. We do not yet understand clearly why structured patterns are obtained from whiskers grown at these high vapor pressures. It may be a whisker-size effect since the main difference caused by the higher vapor pressure should be a different radius and length distribution.

Preliminary experiments studying the heterogeneous nucleation of mercury on tungsten field emitters are in progress. The object of these experiments is to measure the vapor supersaturation required to form a critical nucleus as a function of substrate temperature.

2.24 Field-Emission Studies of the Growth and Oxidation of Single Crystals

W. J. Ambs and E. Escalante,

Corrosion Section

Experiments on the growth and oxidation of magnesium films deposited on tungsten are still in process. So far, rates of surface diffusion and desorption have been measured with established field-emission techniques (Ambs and Escalante in preparation). Multilayer diffusion with a sharp boundary was observed to take place with the activation energy dependent on the crystal face (see Fig. 14). Activation energies around 13 kcal/mole were observed. At higher temperatures, desorption occurred in two stages with

Fig. 13 (100) K whisker field-emission pattern

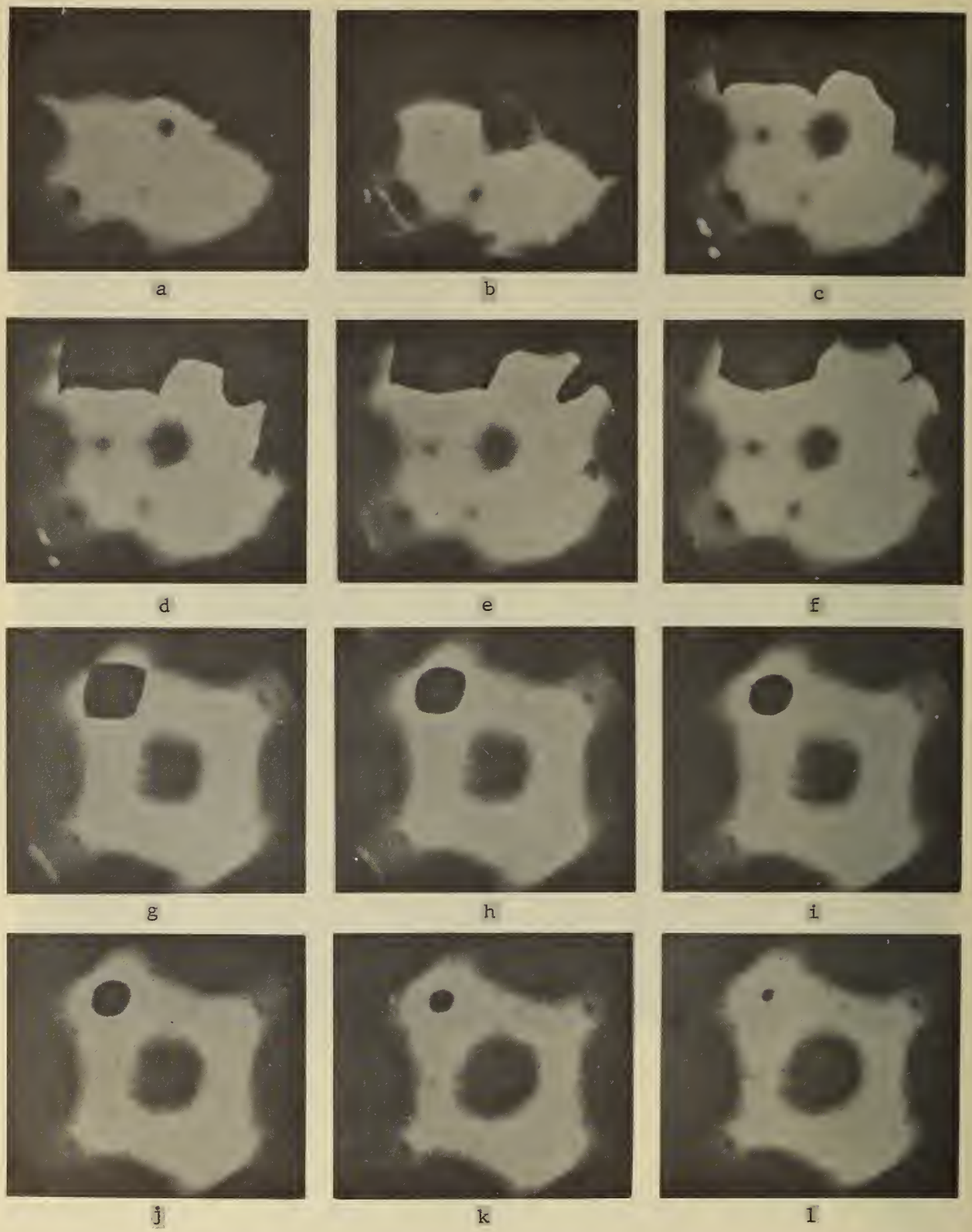

Fig. 14 a: Mg deposit on the side of W emitter; b,c: Migration of Mg around (110) takes place as temperature is raised slightly; d,e,f: Beginning of migration around (100) at a higher temperature; g,h,i,j,k,l: Mg closes around (100)

activation energies of ~34 and 94 kcal/mole. A minimum work function of 3.48 volts was observed. At the end of the first desorption stage this rose to 3.95 volts compared to 4.52 volts for clean tungsten.

2.25 Condensation of Tungsten on a Cold Tungsten Substrate

R. D. Young

Electron Physics Section

A field-ion microscope was used to study the deposition of tungsten onto a liquid-hydrogen-cooled tungsten emitter. Tungsten was evaporated onto one-half of the emitter, and then field evaporated from the surface in small steps. An examination of successive photographs showed that atoms were deposited in a very irregular way, comprising little groups and hills. The photographic evidence together with Monte-Carlo calculations support the assumption that the incident atoms are retained in the first potential well they encounter.

This experiment gives the positions of deposited atoms in atomic detail. It is hoped that this work will stimulate others to exploit the field-emission microscope for the investigation of condensation processes.

3. DEFECT CHARACTERIZATION

Contributions to this chapter are concerned with studies of defect-sensitive properties of single crystals.

3.1 Magnetic Properties of Salt Single Crystals at Low Temperatures

B. W. Mangum,

Cryogenic Physics Section, and

R. P. Hudson,

Heat Division

In addition to the joint effort described below, one of us, B. W. Mangum, has also been producing some rare-earth trichloride crystals. Anhydrous single crystals of lanthanum trichloride, each containing either cerium trichloride, praseodymium trichloride, samarium trichloride, neodymium trichlordie, terbium trichloride, holmium trichloride, or erbium trichloride at a concentration of either 0.2, 0.5, or 2.0 mole percent, have been grown from the melt. The method used was one in which the anhydrous trichloride, sealed off in a quartz tube under one-third atmosphere of helium, was slowly lowered through a furnace with a high temperature gradient.

As a joint effort some of these crystals are being used in an investigation of the spin-lattice relaxation times of Ce^{+3}, Nd^{+3}, Pr^{+3}, Sm^{+3}, Tb^{+3}, No^{+3}, and Er^{+3} ions. The pulsed microwave method is used for measuring the relaxation times. The frequency of the microwaves is 10KMc/sec and the temperatures at which the measurements are made are between 1°K and 4.2°K. Measurements have been made on Sm^{+3} but are not yet complete. The relaxation times for Sm^{+3} show anisotropy with respect to the field direction at the lowest temperatures. Further measurements are in progress.

During the period covered by this report, a paper has been published (Hudson and Mangum, 1963).

3.2 Optical Properties of "Pure" and Impure Crystals, Paramagentic Centers

R. F. Blunt,

Solid State Physics Section

Spectra of a number of systems have been recorded, mainly at room temperature, including: spinel (:Mn); strontium titanate, $SrTiO_3$(:Ti); magnesium fluoride, MgF_2; with X-ray induced color centers; spinel (:Cr); and manganese fluoride, MnF_2(:Co). The emphasis has been on the last material. Besides the "regular" Mn spectrum, the crystals exhibit three broad bands attributable to cobalt, presumably as substitutional Co^{2+}. These bands seen at 6 900, 13 300, and 19 200 cm^{-1} are identified, respectively, as arising from $^4T_1(F) \rightarrow {}^4T_2(F)$, $^4A_2(F)$, and $^4T_1(F)$ transitions. The latter is actually three partially resolved bands at 18 400, 20 200, and ~21 000 cm^{-1}. The simple crystal-field theory yields a Dq of ~800 cm^{-1} and a calculated position of 14 800 cm^{-1} for the $^4A_2(F)$ band. Rhombic distortion of the F^- octahedral cation coordination will depress the $^4A_2$ level since it involves two anions at greater distance than that of the other four, as well as a splitting of the orbital triplet states.

Color centers have been produced in MgF_2 crystals by X-irradiation. So far bands at 27 000 and 40 000 cm^{-1} have been observed and both are easily annealed out at 500°C.

3.3 Laser Microprobe for Analysis of Very Small Samples

B. P. Scribner, M. Margoshes, and S. D. Rasberry,

Spectrochemical Analysis Section

Studies of the laser microprobe, described and illustrated in NBS Technical Note 197, Section 3.10, have continued with particular emphasis on improving the performance of the instrument and in observing the spectra produced by laser excitation of solids. Because of the high energy of the laser pulse, deterioration of several components of the optical system has occurred. The affected portions were the cement layer between components of the microscope used to focus the laser beam, an upper lens component of one objective (cracked), and an interference filter used as an end plate in the laser crystal system (damaged). The objective is now assembled without cement and the manufacturer has replaced the interference filter with a reflector consisting of a stacked array of sapphire plates. The possibility of replacing the glass lens system with a reflecting mirror objective is being considered. Finally, a Mylar cover assembly has been placed over the objective end piece to protect the lens from deposits of sample material ejected by the laser beam.

Observations of the spectra produced by the laser pulse with and without spark cross-excitation have been made by integrating several pulses in each case. For the vapor jet produced by the laser pulse alone the spectra are weak and the spectral lines are highly self-absorbed. With the spark discharge through the jet of vapor produced by the laser pulse, the intensity is increased many times and the spectral lines are reasonably sharp and show little self-absorption. The sensitivity and reproducibility of the latter excitation are being studied. Preliminary observations on zinc-base alloys show that about 0.2 μg of material is vaporized by each laser pulse. By integrating 5 pulses, it was possible to detect 10^{-5}μg of Si, Cu, and Mg as impurities in the zinc sample. This represents a remarkably sensitive level of detection in microanalysis. To assist in improving the reproducibility of the source, techniques are being developed to measure independently the reproducibilities of the flash lamp (which supplies energy to the ruby crystal) and the laser pulse.

The laser has been applied in analysis for the identification of a surface film 3 microns thick, and a metallic grain inclusion, 0.01 mm^2 overall area by 5 microns thick.

3.4 Study of Crystal Defects

D. J. Barber and N. J. Tighe,
Physical Properties Section

Studies of dislocations in crystals of artificial sapphire by means of transmission electron microscopy have been continued. Specimens are thinned with the aid of a device which produces a hot chemical jet (Tighe, 1964). Current work is concerned with dislocations in specimens twisted on the basal plane. A dislocation extending between two etch pits is shown in Figure 15. A hot stage capable of temperatures up to 2000°C is now complete; a tilting hot stage is under consideration.

Crystals of magnesium fluoride, MgF_2, exhibit radiation damage after electron irradiation which produces dislocation loops. This process is being studied with the aid of a cold stage.

In collaboration with E. N. Farabaugh (Crystal Chemistry Section) crystals of rutile have also been thinned for transmission work, and the effects of non-stoichiometry on dislocation behavior will be studied.

3.5 Defects in Thin Oxide Films

J. Kruger, C. L. Foley, and H. T. Yolken,
Corrosion Section

Thin-foil electron microscopy and diffraction were applied to a study of the films formed on iron during potentiostatic anodic polarization. The techniques consisted of anodically polarizing thinned iron foils in boric acid-sodium borate solutions at various passive potentials. By then flooding the surface, while it was at the passive potential, with an inert liquid it was possible to retain the electrochemically formed films so that they could be studied in the electron microscope. Selected-area transmission electron-diffraction studies of these foils offered the advantage that one could study the epitaxial relationship of the oxide with metal substrates of different orientation on a single polycrystalline specimen.

These studies have thus far revealed that the film formed under the conditions described is an oxide with a spinel structure (Fe_3O_4 or γ Fe_2O_3) whose lattice parameter is less than those for bulk Fe_3O_4 or γ Fe_2O_3. This indicates a spinel oxide having vacancies, a possibility suggested by one model of the passive film in the literature. The epitaxial relationships between the oxide and the substrate are now being worked out.

Studies of the existence of strain in thin (~30 Å) oxide films formed on iron single-crystal surfaces at low oxygen pressures have been started. These studies measure by ellipsometry the optical constants in the visible spectrum of the oxide growing on surfaces of different crystallographic orientations. We hope to detect variations in epitaxially induced strain on oxides growing on substances of differing orientation by observing the effects of this strain on the position of the absorption peaks of the oxide.

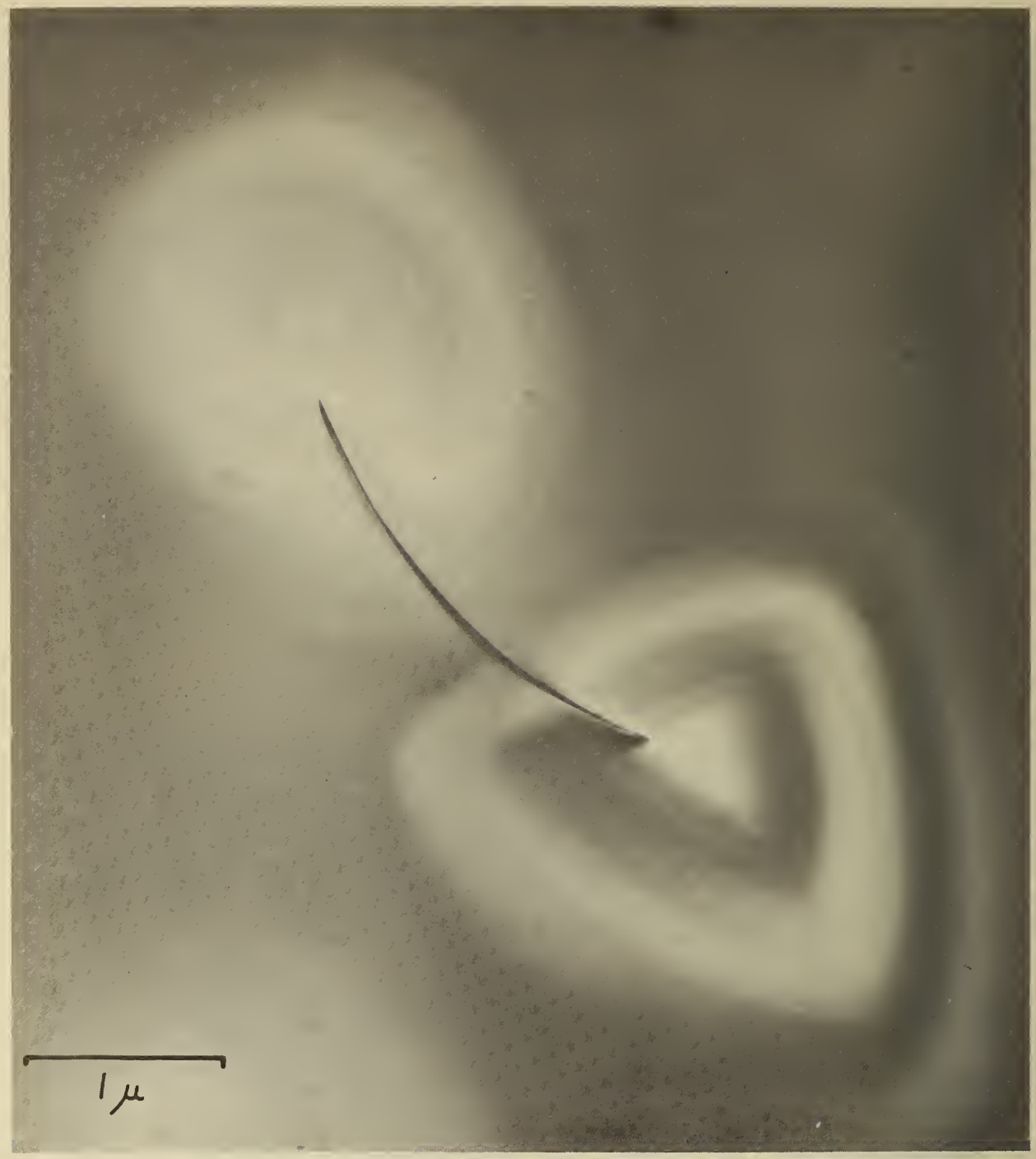

Fig. 15 Electron transmission micrograph of a chemically thinned {0001} section of artificial ruby. A short dislocation segment is shown terminating at the centers of two etch pits, both on the same surface

3.6 Effect of Point Defects on the Dynamic Properties of Crystals

J. B. Wachtman, Jr., and S. Spinner,

Physical Properties Section

Elastic and electrical properties are being studied as a function of temperature and frequency, and the results interpreted in terms of chemical impurities and related point defects.

Mechanical and electrical relaxation occurring in thoria, ThO_2, containing up to 1.5 mole percent calcium oxide, CaO, has been interpreted in terms of oxygen vacancies trapped by Ca ions (Wachtman, 1963). The investigation is being extended to cover a wider range of frequency and composition dependence. The model will thus be subjected to more stringent tests after it has accounted satisfactorily for the previously obtained observations.

The study of Ni-doped rutile has yielded two internal-friction peaks which may be associated with isolated as well as with paired Ni ions. Earlier work on vacuum-reduced rutile (Wachtman and Doyle, 1964) appears to be consistent with this interpretation. Further insight into ionic movements in rutile could be obtained by studying internal friction associated with oxygen-vacancy motion. Such vacancies should exist in chromium-doped rutile and suitable specimens are being prepared.

Previous work on relaxation processes by this project has been interpreted in terms of a nearest-neighbor model. A model including neighbors out to second nearest was published by Franklin (1963). Franklin's approach has been applied to two types of paired point defects including neighbors out to third nearest (Franklin, Shorb, and Wachtman, 1964).

3.7 Crystal Symmetry and Crystal Properties

J. B. Wachtman, Jr.,

Physical Properties Section, and

H. S. Peiser,

Crystal Chemistry Section

The effect of crystal symmetry upon physical properties continues to be a fruitful field of investigation despite the extensive treatment by Voigt many years ago. The revived interest stems in part from the discovery of new properties unknown to Voigt and in part from the realization that space-group symmetry is important for some properties despite the fact that the classical treatment deals only with point-group symmetry.

The types of point defects which can cause internal friction and the type of stress required have been determined for many of the common refractory-oxide structures as reported previously in NBS Technical Note 197, Section 3.5.

A systematic scheme of all possible subgroups reached by the action of homogeneous stress has been reported for all 230 space groups by Peiser, Wachtman, and Dickson (1963). This tabulation is expected to be useful in studying other properties in addition to internal friction. Possible applications include the splitting of magnetic-resonance spectra under stress and the classification of symmetry changes associated with solid solution.

A tabulation is being made for the centrosymmetric space groups showing the mapping of all the special positions of a given group onto the special positions of each of the space subgroups which can be reached by homogeneous

stress. This should be a useful addition to the space-group reduction tables mentioned above.

3.8 Dislocations in Metals by Electron Microscopy

A. W. Ruff, Jr.,

Lattice Defects and Microstructures Section

A study of dislocations in low stacking-fault energy materials has been initiated. Transmission electron-microscope observations on extended dislocations should permit the determination of the stacking-fault energy and its variation with alloy composition. Initial results on extended nodes in 302 stainless-steel foils have been obtained. The rare observation of a single-ended Frank-Read source in operation has been made (Fig. 16).

3.9 Growth of Helical Dislocations

R. deWit,

Lattice Defects and Microstructures Section

The abstract of a paper published during the reporting period follows (deWit, 1963):

"Conclusions reached in a paper by Weertman [Trans. Met. Soc. AIME, 227, 1439 (1963)] are amplified in a mathematical and graphical way. It is shown that in a stressed crystal, a straight dislocation may be in a position of unstable equilibrium with respect to helix development, and how a small perturbation may start the dislocation off on its helical path. Helix development occurs by diffusion; bulk diffusion is necessary for development from a screw, but core diffusion is sufficient for development from an edge dislocation. For a mixed dislocation helix development can take place by core diffusion if the helix also climbs; a diffusion reversal takes place when the slope of the helix equals the slope of the Burgers vector. The work done on a crystal by the external forces is graphically shown to be consistent with the direction of motion of the dislocation in helix development. Finally, a detailed mechanism for tangle formation from helices is presented. In the course of helix development, a glide situation may be reached where a segment of each helix loop lies in a slip plane in which it can expand by glide. Thus is it visualized how a helix can deteriorate into a tangle."

3.10 Characterization of Electrodeposited Crystals

F. Ogburn and A. deKoranyi

Electrolysis and Metal Deposition Section

Copper dendrites are easily formed by electrodeposition from cuprous chloride solutions. These often take the form of flat tree-like structures with the branches and trunk all in one plane. X-ray diffraction and metallographic examination of a few such dendrites show that a growth twin extends throughout the branches and trunk of these dendrites (Fig. 17). The absence of three-dimensional branching is clearly associated with the presence of a growth twin which has a marked influence on the growth of an electrodeposit.

Examination of electrodeposited lead dendrites, which are also flat, shows them to contain flat voids or channels, and to be oriented with {111} planes parallel to the overall dendrite or platelet. At least two orientations of the lead are always present. These sometimes have a normal twin relationship but may have a rotational relationship other than the 60° of the twin structure. These dendrites are being investigated further with

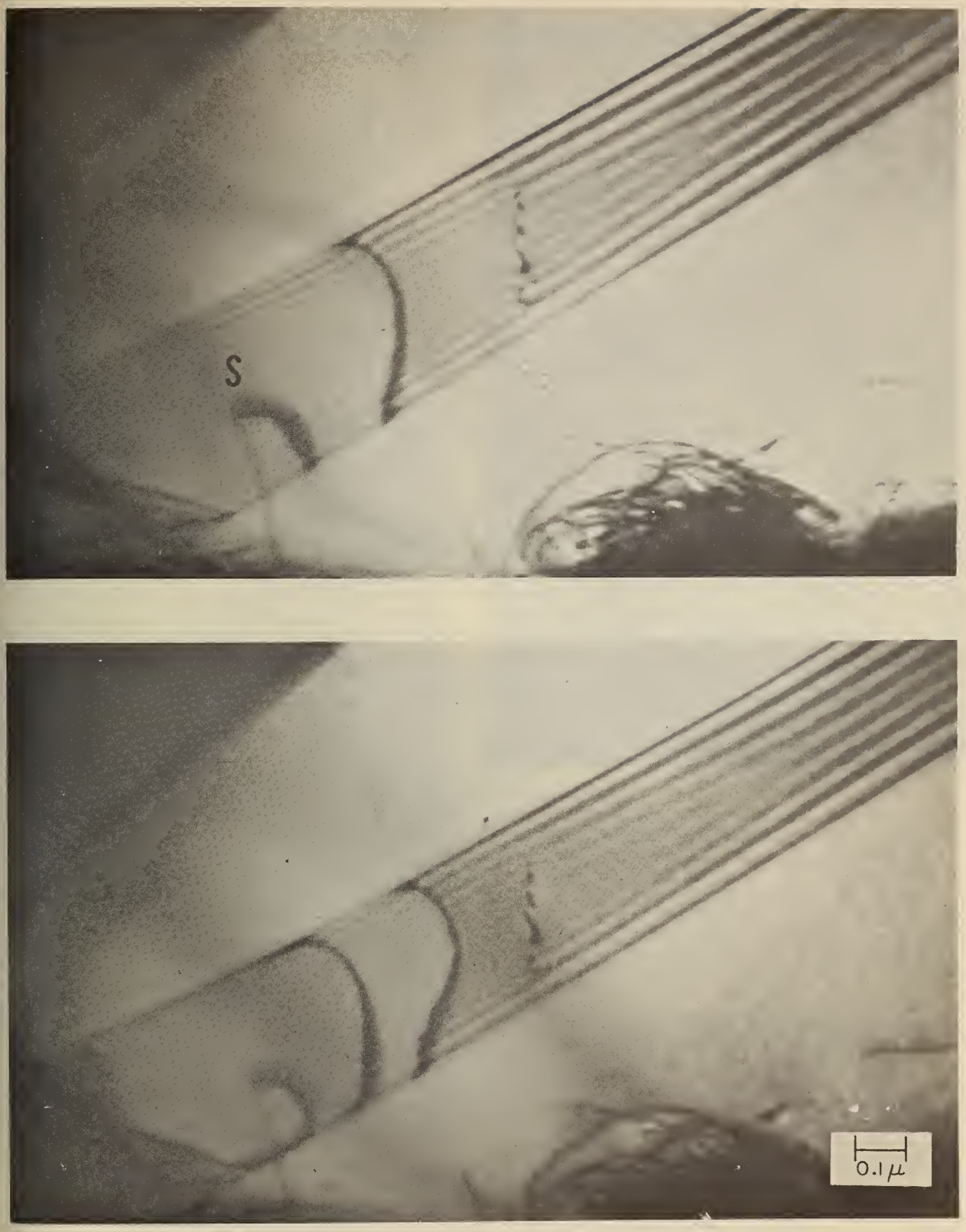

Fig. 16 Transmission electron micrographs of a single-ended Frank-Read source (s) in operation. Sample is 302 stainless-steel foil approximately 2000 Å thick

Fig. 17 Section of copper dendrite showing twin boundary

respect to the angular relationship of the crystals making up the dendrites and to the crystallographic direction of their growth.

3.11 Second-Order Twinning in Aluminum

T. H. Orem,

Corrosion Section

In a continuing study of the corrosive behavior of aluminum, a number of instances of twinning have been observed in specimens prepared for this purpose. An especially noteworthy example, showing incontrovertible evidence of second-order twinning in aluminum, is shown in the accompanying photograph of a twinned aluminum rod (Fig. 18).

The two grains immediately within the elliptically shaped boundary are twinned with respect to that part of the rod outside this boundary. The two grains are thus first-order twins with respect to the latter. The wedge-shaped grain is twinned with respect to the above two grains at both the straight and jagged boundaries of the wedge. Thus the wedge-shaped grain bears a second-order twin relationship with that part of the crystal outside the elliptical boundary.

3.12 Accurate Measurement of the Fundamental Electrical Properties of Semiconductor Crystals

J. C. French, L. J. Swartzendruber, G. G. Harman, and

H. A. Schafft,

Electron Devices Section

Extensive calculations were completed which were related to the solution of a number of electrical potential problems arising from two- and four-point probe measurements on a variety of single-crystal sample shapes. Non-uniformity of resistivity and errors in probe placement or sample size were considered.

Although generally conceded to be less accurate than the two-point probe method outlined in Section 3.6 of NBS Technical Note 197, the four-point probe is by far the most widely used device for the measurement of resistivity of semiconductor single crystals. It provides a simple, non-destructive test and is therefore of great industrial and scientific importance. A significant industrial concern over the use of four-point probes to determine the uniformity of resistivity of silicon wafers, together with the desire to use this simple technique to screen samples for the more accurate but more time consuming two-point probe measurements in the work of this project, led to the current emphasis on these calculations.

The results have been the determination of the correction factors for four-point probes on rectangular parallelepiped samples with plated ends (permitting the comparison of two- and four-point probe measurements for calibration purposes) the correction factors for four-point probe measurements as a function of position on thin circular wafers, the disclosure of the limits of the ability of the four-point probe to detect regions of non-uniform resistivity, and the relation of the measured non-uniformity to that actually present (Swartzendruber, 1963). Tables of the numerical values required in each case have been prepared through use of the 7090 computer, and publication of the results is proceeding. A few samples are shown in Figure 19.

The four-point probe can be used to eliminate grossly non-uniform samples, but in order to measure the variation in resistivity with greater

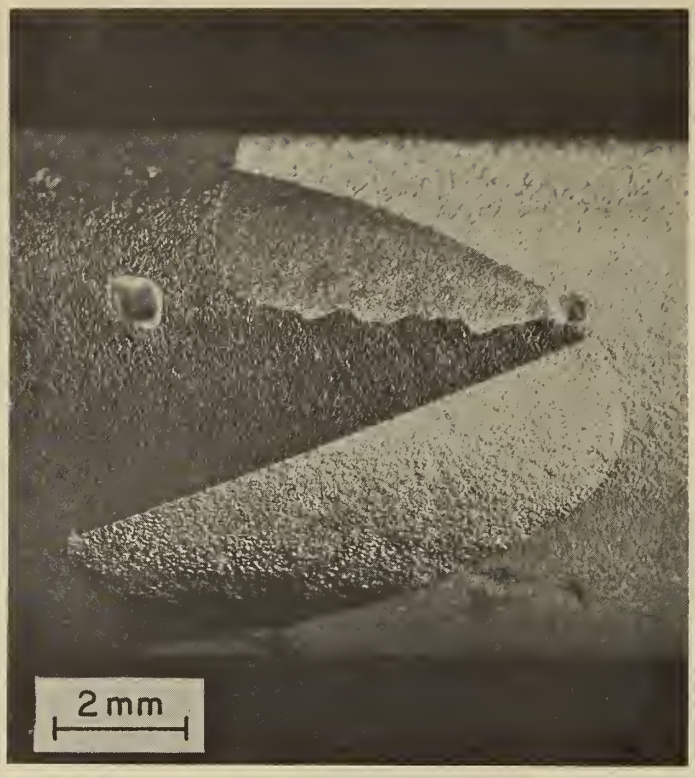

Fig. 18 Al twin

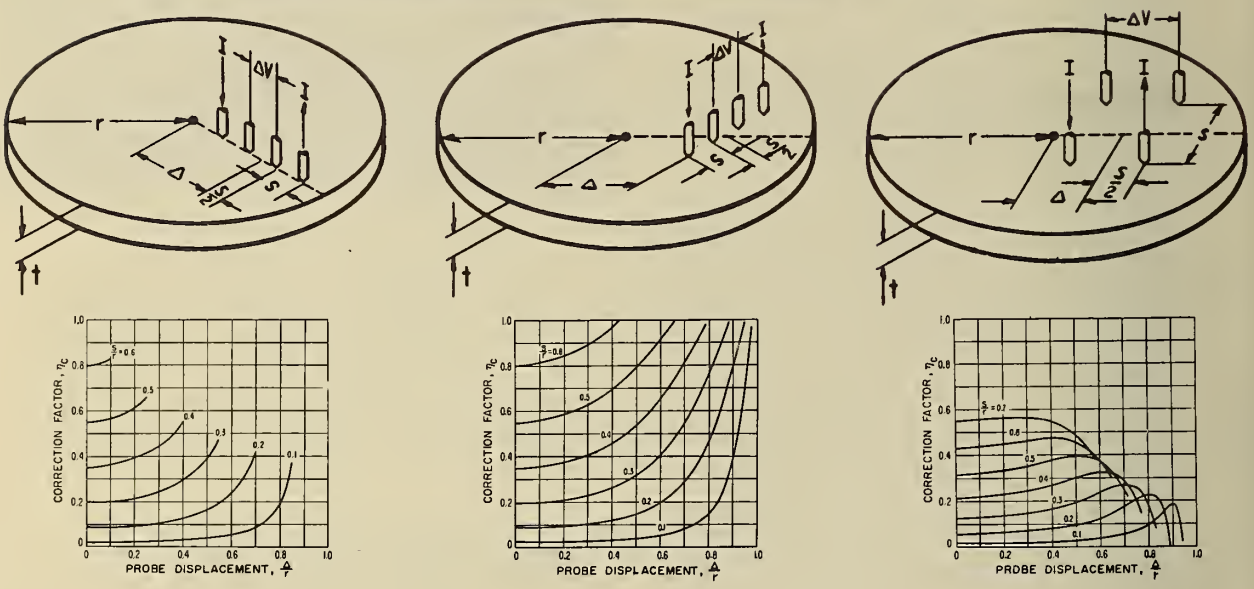

(a) In-line array displaced along a radius

(b) In-line array displaced perpendicularly to a radius

(c) Displaced square array

Fig. 19 Correction factors for three arrangements of four-point probes on thin circular semiconductor single-crystal samples plotted against probe displacement. The correction factor, η_c, relates the apparent resistivity, ρ_o (calculated from the usual expressions appropriate to the in-line or square array) to the true resistivity of the sample ρ, in the expressions:

$$\rho = \rho_o/(1+\eta_c)$$

linear resolution, and yet rapidly, a machine for photovoltaic probing has been completed and is awaiting evaluation. It will scan a sample at rates up to about one centimeter per minute to yield a meter reading or, upon calibration, a plot of resistivity vs. length on an x-y recorder. Sample preparation techniques, though not fully developed, have already advanced to a point which makes the high-resolution scanning possible. The samples so far measured by manual probing have shown that non-uniformity of resistivity will be of major concern in this work.

The work on second breakdown in transistors mentioned in Section 3.6 of NBS Technical Note 197 (project leader H. A. Schafft) has continued with the application of temperature-sensitive phosphors to detect the location of the breakdown site before excessive damage to the transistor has occurred. It has been possible to show that structural irregularities are important to the development of second breakdown (Schafft and French, 1963). Work concerned with the identification and role of crystal defects in producing these structural irregularities as well as influencing the development of second breakdown will now begin.*

The continuing investigations of electroluminescence (project leader G. G. Harman) have been concerned primarily with the spectral emission characteristics of materials such as ZnS and CdS with various impurity levels and under such excitation as ultra-violet light and electron bombardment. The effects of the ambient atmosphere on electroluminescence have also been studied empirically, with polycrystalline powders being used to increase the surface to volume ratio. Most of this work was done at the University of Reading in England under an NBS training program.

There have recently been published some additional results from the now concluded studies of muscovite mica (Ruthberg, 1963).**

The solid-state technology project (J. C. French, project leader) has devoted a major part of its effort to work on silicon single-crystal nuclear-particle detectors, devices which have had a major impact on high-energy particle studies because of their excellent energy resolution and convenient size and operating characteristics.

3.13 Crystal Characterization by Diffraction Topography

R. D. Deslattes,

Crystal Chemistry Section

The double-crystal diffraction apparatus, plans for which were discussed in NBS Technical Note 197, Section 3.7, was completed and placed in operation in September. Its precision has proved equal to the expectations indicated in the former report. A considerable amount of exploratory work has been carried out, and the following results are noted.

The first investigation concerned questions of method. Previous double-crystal work has been restricted to the case of symmetrical reflection from pairs of identical crystals in dispersive (+,+) and non-dispersive (+,-) configurations. The former case is limited in sensitivity by the large natural width associated with characteristic X-ray lines. The latter configuration gives rise to multiple and/or diffuse images (owing to the inevitable lack of spectral purity in the source) unless slits and large diffraction

---

* This work was supported in part by the Rome Air Development Center.

** This work was supported in part by the General Services Administration.

Fig. 20 Double-crystal diffraction topograph from a pair of natural quartz specimens. The samples were cut parallel to a set of {1120} planes, ground, polished, and etched for 20 minutes in 35% HF

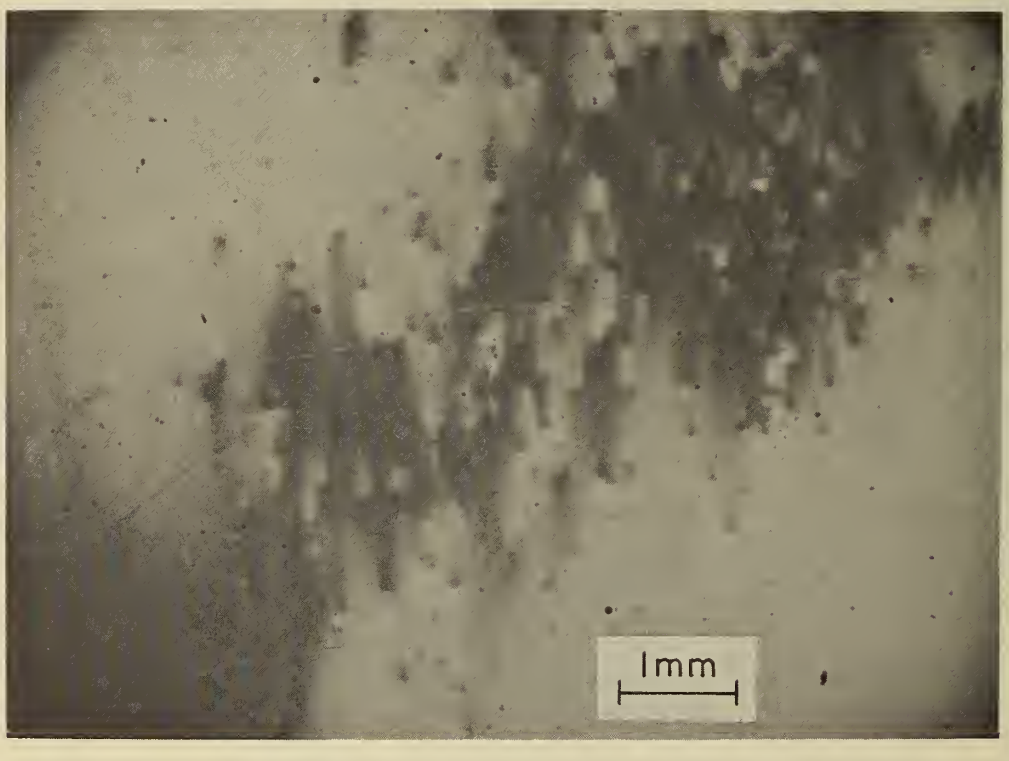

Fig. 21 Double-crystal diffraction topograph of sample of KAP analyser crystal. The reference crystal was ADP (101) and the spectrometer configuration (2,-5)

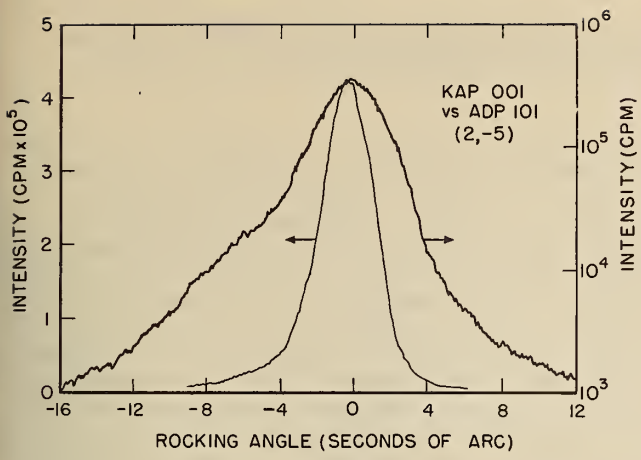

Fig. 22 Rocking curve (2,-5) for the pair of crystals used in obtaining Fig. 21. The logarithmic intensity scale allows study of the remote tail regions

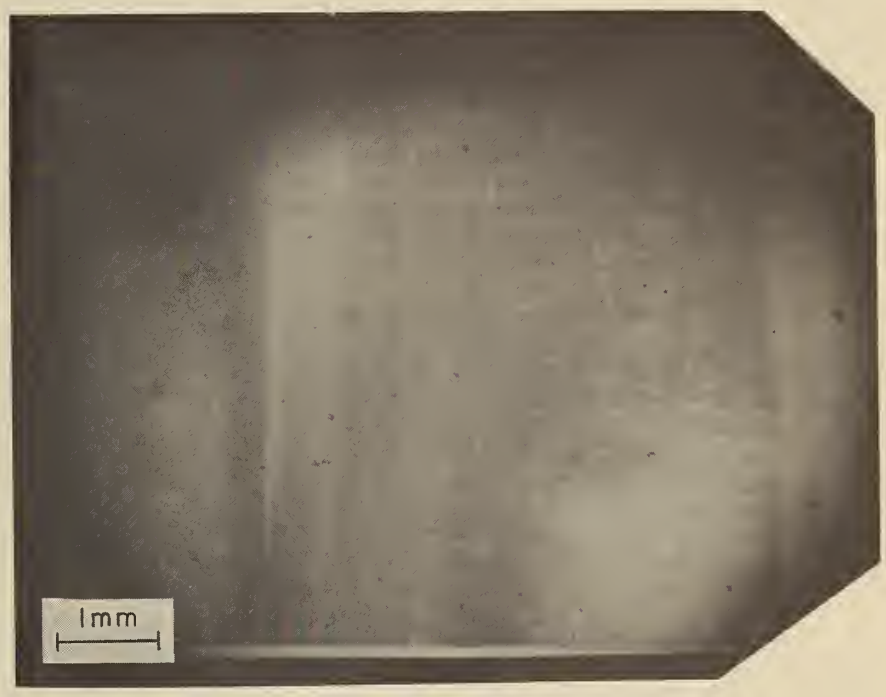

Fig. 23 Diffraction topographs from a pair of ADP (101) crystals. These had been string sawed and chemically polished. The image doubling is due to undispersed alpha doublet. Although the significant long-range strain appears, there are some regions free of the small images which are tentatively identified as emergent dislocations

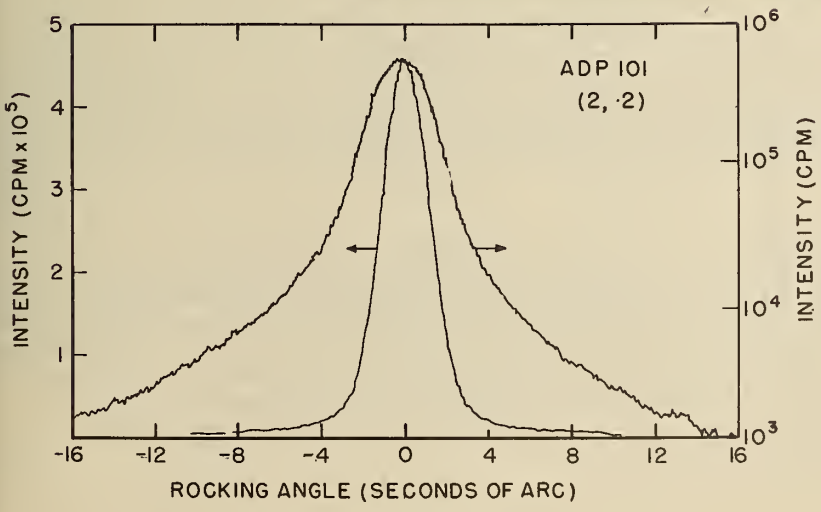

Fig.24 Rocking curve (2,-2) for the pair of crystals used in obtaining Fig.23

angles are employed. In this case, only a small part of the crystal can be explored without scanning, and one of the more attractive features of the double-crystal arrangement is eliminated.

In an attempt to avoid these difficulties, the negative orders of double diffraction from crystals having almost equal interplanar spacings have been especially investigated. The total dispersion in this case is the difference of the dispersions for the two crystals. If this difference is sufficiently large so that the α-doublet separation exceeds the combined Darwin widths for the two crystals, the doublet is resolved and no restriction of horizontal divergence is required to secure unique imaging. This result requires only that the lattice constants differ by more than a few parts in ten-thousand — a condition which obtains rather often for crystals of different species. On the other hand, if a match within about 10% is obtained, then the contribution of spectral-line width to the rocking curve does not exceed that due to the diffraction process itself. Hence, a sensitivity within a factor of two of the maximum attainable is realized. There is, of course, a considerable and desirable gain of intensity in the (+,-) configuration relative to that in the (+,+) configuration. Double-crystal diffraction topographs taken from calcite crystals with copper, K_α, and tungsten, L_α, radiation in the above configurations confirm these elementary expectations.

In addition to the above investigation of method, several groups of crystals were studied. These included specimens of natural quartz and calcite, specimens of solution-grown ammonium dihydrogen phosphate, ADP, and potassium acid phthalate, KAP, and specimens of melt-grown germanium and silicon.

Natural quartz specimens of high spectroscopic quality were obtained commercially. In addition to defect images which appeared similar to those reported by other investigators, several specimens exhibited topographs resembling a class of visual aurora as shown in Figure 20. In the case of one pair, etching for 20 min. in 35% HF did not alter the image. The effect is not understood at present; however, it may be conjectured to be analogous to the well known strain effects of segregated point defects. These have been, in the case of synthetic crystals, associated with irregularities in growth conditions. In the case of the natural-quartz crystals, the analogous irregularities may be associated with geological epochs. Somewhat similar effects have been observed in specimens of natural New Mexican calcite.

The synthetic crystals investigated were solution grown by temperature-program techniques. One family consisted of KAP crystals obtained commercially. The object in this case was to find crystals suitable for long-wavelength X-ray spectroscopy. The results, as typified in Figure 21, indicate that spectra recorded by such crystals would be of dubious validity at best. The crystals exhibit both local defects, presumably dislocations, and long-range strain fields which together result in less than one tenth of the crystal reflecting at any one angle. As shown in Figure 22, the corresponding rocking curves [versus a relatively perfect ADP (101) reference] also indicate the futility of attempting to apply such crystals to problems in precise spectroscopy.

The second family of synthetic crystals consisted principally in (101) cuts of ADP (see NBS Technical Note 197, Section 2.5). The major part of this investigation was found to be concerned with techniques of surface preparation (see Section 2.8 of this Technical Note). Results obtained after moderate improvement in preparation technique are indicated by the topograph in Figure 23. The corresponding rocking curves appear in Figure 24. These suggested the possible utility of suitably prepared ADP specimens for long-wavelength X-ray spectroscopy. Results obtained at 8.3 Å are given elsewhere in this report (see Section 3.18).

3.14 Automation of Single-Crystal X-Ray Diffraction Intensity Measurements

F. A. Mauer,

Crystallography Section

The importance of automatic equipment in obtaining accurate measurements of single-crystal diffraction intensities for studies of crystal perfection and for structural analysis was pointed out in NBS Technical Note 197, Section 3.13. Current plans call for the automation of an existing X-ray diffractometer and single-crystal orienter to be carried out by a commercial firm in two steps. The first step (to be completed by July, 1964) involves fitting the three shafts of the manual device with shaft encoders and motors so that the shaft positions can be read and set with an accuracy of ± 0.01° by an operator at a remote console. On a command from the operator, the final setting of each shaft is to be recorded on punched-paper tape and on a printer. Likewise, the number of counts registered by the scaler in measuring background and peak intensities is to be recorded.

The second step (to be completed later) involves the addition of a programmer, a block-tape reader, and a comparator so that the machine will be capable of reading commands from a punched-paper tape, making the necessary settings, and recording the data, all without human intervention.

3.15 X-Ray Studies

M. I. Cohen,

Solid State Physics Section

The crystals now being studied include those mentioned in Technical Note 197, Section 2.2, and in addition sodium azide, NaN_3; potassium azide, KN_3; and cadmium sulfide, CdS. A survey of the major misorientations present in a Verneuil-technique-grown crystal of rutile, TiO_2, is under way (compare Section 2.7). The crystal was grown at a rate of approximately 1 cm per hour. Incomplete results indicate an average sub-grain size of about 2 mm. The "c"-axis deviation between grains is about ± 1°, and the rotation around the "c" axis is ± 2°.

3.16 High-Voltage Laue Photographic Inspection of Large Single Crystals

B. Paretzkin and H. S. Peiser,

Crystal Chemistry Section

This method (see NBS Technical Notes 174, Section 5.13, and 197, Section 3.14) has been shown to be suitable for revealing misorientations and strain in thick crystals, even while they are enclosed in a vacuum system or a furnace (Paretzkin and Peiser, in preparation). The authors are ready to collaborate with anyone wishing to characterize crystals under such conditions.

The most interesting aspect for further work is the coherence observable over cyrstal distances of the order of 1 cm. In this respect the method is very sensitive to regional crystal misalignments of only a few seconds of arc.

3.17 Chemical Purity by Dielectric Cryometry

G. S. Ross and L. J. Frolen,

Analytical Chemistry Division

In Section 5.18 of NBS Technical Note 174, a new method was described in which the dielectric constant was measured in conjunction with the change in temperature as the sample melted. From the data obtained the chemical purity can be calculated with high precision. These studies have been completed (Ross and Frolen, 1963).

3.18 Optical Properties of Cadmium Sulfide and Telluride*

L. H. Grabner and R. C. Keezer,

Solid State Physics Section

Irradiation of undoped cadmium sulfide, CdS, platelets just to the long-wavelength side of the absorption edge produces a decrease of the photocurrent (quenching) due to radiation on the short wavelength side. Noteworthy characteristics are: (1) Quenching spectra, measured hitherto at the temperatures 293°K, 205°K, and 94°K, duplicate the spectra of the blue-edge photoluminescence [Pedrotti and Reynolds, Phys. Rev., 120, 1664 (1960)] (except for luminescence due to the simultaneous emission of a photon and a phonon, the analog of which is absent in the quenching spectra). The quenching spectra are sensitive to radiation polarized parallel or perpendicular to the c-axis in the same manner as the luminescence is polarized. (2) When the sample is irradiated with constant intrinsic light, photocurrent versus voltage shows an ohmic region followed by a saturation range. This presumably is due to hole injection [Lampert, Phys. Rev., 125, 126 (1962)]. Quenching is observed only in the saturation region and its magnitude is a function of the voltage. Contacts are of melted indium.

3.19 Irradiation Studies

M. I. Cohen,

Solid State Physics Section

Crystals of magnesium fluoride, MgF_2, have been irradiated by X-rays in connection with a study of color centers (see report by Blunt, Section 3.2). Accelerating potentials of 50, 140, and 250 kV were used. Analysis of the optical absorption spectra showed that centers had been produced and that the 50 kV radiation was slightly more efficient in the production of these centers. Total dosage per sample was on the order of 50,000 roentgens.

A specimen of MgF_2 was irradiated by 100 kV electrons in an electron microscope. Examination with an optical microscope showed an area of $< 1 mm^2$ colored yellow-green. Optical absorption data could not be obtained due to the small size of the spot.

3.20 Development of an Adiabatic Solution Calorimeter

D. D. Wagman,

Thermochemistry Section

An adiabatic high-temperature solution calorimeter (see NBS Technical

---

* This work was supported by the Office of Naval Research

Note 174, Section 5.4) has been completed and assembled. Preliminary trials to test the vacuum tightness of the assembly and to determine the efficiency of the stirring and of the sample-holding mechanisms are under way. After this the thermocouple leads that operate the shield controls will be installed, at which time the apparatus will be ready for adiabatic operation.

It is anticipated that for maximum attainable precision, an additional control system to regulate the temperature at the top of the shield will have to be installed, but the purchase of the necessary electronic equipment has been temporarily postponed.

4. CRYSTAL PHYSICAL PROPERTIES

Contributions to this chapter are concerned with the physical properties of crystals which do not depend primarily upon the degree of crystal perfection or whose dependence on that perfection is not the principal aim of the investigation.

4.1 Reference Data on Single-Crystal Elastic Constants

J. B. Wachtman, Jr., S. Spinner, and
R. W. Jackson,
Physical Properties Section

Elastic constants of inorganic single crystals are being determined as a basic physical property when suitable crystals become available. The elastic constants of uranium dioxide, UO_2, at 25°C were determined by Wachtman, Wheat, Anderson, and Bates (1964). Work is now under way on a determination of the temperature dependence of the elastic constants of rutile over the range 25°C to 600°C. A crystal of thoria, ThO_2, has been obtained and collaboration with P. M. Macdeo of the Glass Section is planned to determine the elastic constants by an ultrasonic technique.

Experimental capabilities are being enlarged by the construction of a Schaefer-Bergmann apparatus for the measurement of elastic constants. In this apparatus, ultrasonic standing waves are used as a diffraction grating for monochromatic light.

4.2 Deformation and Fracture of Ionic Crystals

S. M. Wiederhorn,
Physical Properties Section

The surface energy of solids is an important factor which influences the breaking strength; yet surface energy is difficult to determine, particularly for surfaces which are not cleavage planes. A technique for making such determinations by use of a modified Gilman-Westwood method is being investigated with glass for the exploratory measurements. In this technique, a crack is propagated in stages; the plane of propagation is controlled by a scratch inscribed before the test. Early results on glass give reasonable values of the surface energy.

4.3 Studies in Solid-State Theory

A. H. Kahn,
Solid State Physics Section

A tight-binding calculation of the electronic energy bands of strontium titanate, $SrTiO_3$, has been completed. The over-all picture is that of a conduction band derived from Ti-3d states spread to a width of ~4 eV by σ-bonding with the O-2p states, and with smaller splittings by cubic crystalline fields and π-bonds. Similarly, the valence bands are derived from O-2p states spread by a large σ p-d bond, a smaller π p-d bond, and smaller splittings by axial crystalline fields and σ and π bonds between the oxygen ions. The over-all valence bandwidth is ~4 eV.

The calculated band structure is in satisfactory agreement with experiments relating to conductivity, Hall effect, thermoelectric power, and X-ray emission. The experimental and theoretical results were reported at the Buhl Conference in Pittsburgh (Kahn, Frederikse, and Becker, 1963). The theoretical analysis, together with a qualitative discussion of a similar calculation for rutile, TiO_2, will be submitted to the Physical Review.

4.4 Electronic Transport

H. P. R. Frederikse, J. H. Becker,
W. R. Hosler, and W. R. Thurber,
Solid State Physics Section

Investigation of the lower-lying conduction bands in rutile by measurements of the Hall coefficient and electrical conductivity is nearing completion. It has been established that for temperatures above 40°K appreciable conduction in more than one band takes place. Analysis in terms of two bands leads to an energy separation of the band minima of approximately 0.05 eV. Work is in progress to determine parameters describing these bands (effective masses, location of the minima, etc.) and scattering mechanisms (mobility, i.e. electron-phonon and electron-impurity interactions). From the work one may also conclude that reduction of rutile leads to several types of lattice defects.

A method was developed to obtain low resistance metal-semiconductor contacts by use of localized pulsed heating, with best results achieved with a ruby-laser beam.

The conductivity and the Hall and Seebeck coefficients of reduced and doped strontium titanate, $SrTiO_3$, were measured over the temperature range 4.2-300°K. An average effective mass of (6-16) m_o was deduced from these experiments. This value agrees well with the results of a recent energy-band calculation for $SrTiO_3$ based on a tight-binding approximation (see A. H. Kahn, Section 4.3). One can also conclude that the original impurity level of the $SrTiO_3$ crystals is of the order of (1-2) x $10^{18} cm^{-3}$. Introduction of donors (Ti^{3+}, Nb^{4+}, etc.) below this level gives rise to strong compensation.

4.5 Hall-Effect Measurements*

S. Rubin,
Engineering Electronics Section

The initial objectives of this project were the establishment of standardized terminology and measuring methods for Hall-effect generators and related devices. The objectives have now been expanded to include magnetoresistive devices.

---

* This work was supported by the Bureau of Naval Weapons.

Two new sensitivity indices for Hall generators, one a function of control current alone and the other a function of magnetic induction alone, have been proposed and are included in the Hall-generator standard referred to in Section 4.3 of NBS Technical Note 197. The new indices are useful for small signal as well as static applications of Hall generators.

Work was begun on a standard of definitions, terminology, letter and graphic symbols for magnetoresistive devices. Initial contact has been made with manufacturers of magnetoresistive devices, and a first draft of proposed standards in this area will be circulated in the early part of 1964.

Work in the area of instrumentation for electron paramagnetic-resonance magnetic-induction measurements was suspended for most of this period, but will be resumed in the early part of 1964.

4.6 Dielectric and Mechanical Properties*

J. H. Wasilik,

Solid State Physics Section

As a continuation of our investigations of the lattice properties of single-crystal lead fluoride, PbF_2 (cubic, CaF_2 structure), we are measuring the room-temperature elastic constants of this material using a pulse-echo technique. This work is being done in collaboration with the Physical Properties Section of the Inorganic Solids Division. Present results are $C_{11} = 8.88 \pm .1$, $C_{44} = 2.45 \pm .03$, and $C_{12} = 4.72 \pm .11$, all x 10^{11} dynes/cm^2.

A recent report indicated phase changes in NaN_3 at 19°C. This conclusion resulted from analysis of electron paramagnetic resonance and X-ray spectra [Miller and King, J. Chem. Phys., 39, 2779 (1963)].

In collaboration with R. Forman of the Section, we have looked for anomalies in the dielectric properties (dielectric constant and dielectric loss) of single-crystal sodium azide, between room temperature (25°C) and -10°C; we have concluded that anomalies of ~3% or greater do not exist in this temperature region when the measuring electric field is in the c direction.

We did discern that the capacitance and loss of NaN_3 were quite sensitive to humidity variations, exhibiting responses to humidity increases with response times of the order of seconds. Further investigations of these properties are planned.

4.7 Dielectric Properties of Semiconductors

E. C. Bamberger and J. L. Dalke,

Radio and Microwave Materials Section

As described in Section 5.7, Bienenstock and Burley (1963) have found that the thermal expansion of a phase of silver iodide, AgI, with a zinc-blende structure is negative to approximately 80°K, positive in the range of 80° to 110°K, and then attains a constant negative high-temperature value. This apparently unique and primarily negative thermal expansion in the large temperature range from 4.2° to 300°K for cubic AgI was determined from lattice-constant measurements by means of X-ray diffraction techniques.

---

* This work was supported by the Atomic Energy Commission.

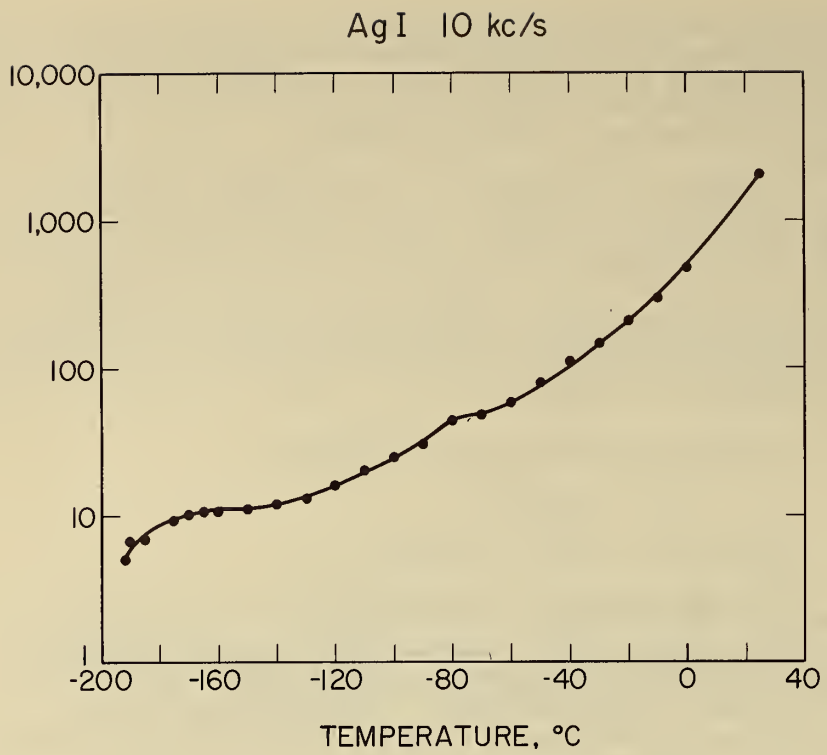

Fig. 25a Dielectric constant of silver iodide plotted against temperature at 10 kc/s

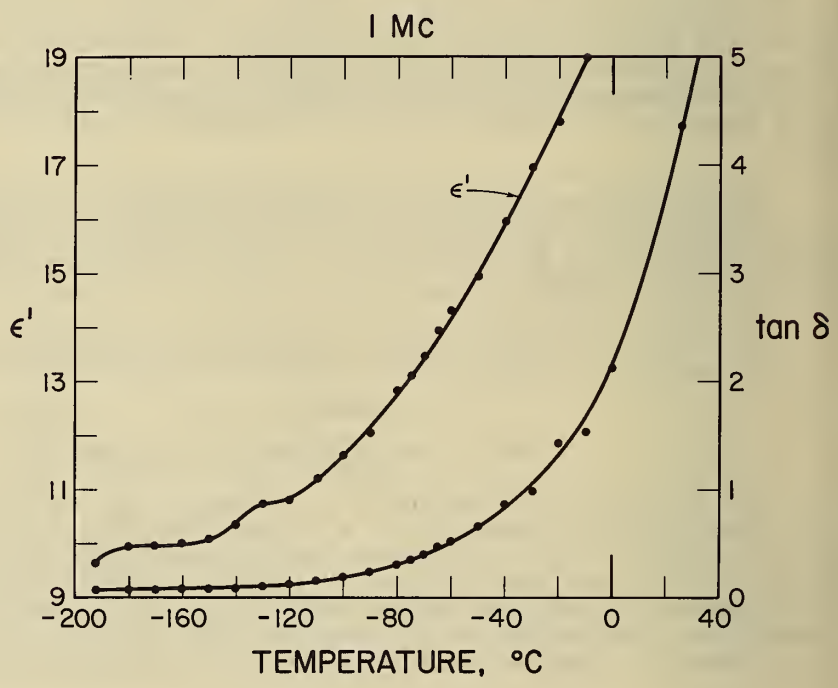

Fig. 25b Dielectric constant of silver iodide plotted against temperature at 1 Mc

The expansion is explained in terms of a model which shows the dependence of thermal expansion on structure and bonds. The authors discuss the primary role of covalency and its contribution to the low-temperature contraction. The particular form of the interatomic interaction appears to contribute primarily to the balance between optical and acoustical modes. In the case of AgI it is the large n in the nearest-neighbor repulsive interaction, r^{-n}, which accounts for the negative high-temperature limit. The positive thermal expansion at intermediate temperatures is the result of transverse optical modes with frequencies lower than the frequencies of the transverse acoustical modes.

The purpose of the present investigation is to determine the dielectric relaxation spectrum of AgI and to see if there is any correlation with the thermal-expansion observations. Measurements of the complex dielectric constant show an inflection point in the dielectric-constant versus temperature curve in the same range where the thermal expansion becomes positive (see Fig. 25, a and b). Rather large dielectric-constant values were observed. These have not yet been explained. Cubic AgI is not available in single-crystal form. It is thus possible that these large values may come about from interfacial polarization in the polycrystalline specimens. However, it is also possible that the mobile Ag ions encounter a potential-well structure which is not yet understood.

4.8 Crystals of Organic Molecules

R. A. Keller and D. E. Breen,
Physical Chemistry Division

The objectives of this new project are to study the properties of the triplet state and the weak intermolecular interactions in crystals of organic molecules.

The process of transfer of electronic excitation from one state to another is important in the fields of biological activity, electrical conductivity, photosynthesis, and laser technology. In both biological activity and photosynthesis, the system absorbs energy in one place and transfers this energy to another form in another place. Information is needed on the basic mechanisms of such transformations. The interest in the use of organic molecules in lasers and photoconductors is the result of the ease of changing the physical properties of these molecules by chemical substitution. The weak interactions between molecular units are in contrast to most of the previous work in solid-state physics which was concerned with systems with strong interactions between their fundamental units. In molecular systems, good approximation to the initial and final states of the system undergoing energy migration are the zero-order states of the isolated molecular unit. These states are connected by small perturbations either inherent in the isolated molecule and modified by the solid environment or caused entirely by the solid environment. We will study these states and the nature of the small perturbations.

In particular, we are interested in the intermolecular and intramolecular properties of the triplet state. Triplet states are populated by radiationless transitions from optically excited molecular singlet states. We will study triplet-state properties such as its lifetime, rise time, temperature effects, solvent effects, polarization, quantum yield, and extinction coefficient. From these properties, we can derive information on the perturbations which connect the spin-orthogonal triplet and singlet systems. Triplet excitations have been shown to migrate from molecule to molecule. This process gives rise to impurity trapping of excitation and to a phenomenon called delayed fluorescence (the process of two excited molecules interacting) which results in bimolecular quenching of the triplet state and in the production of molecules (in excited singlet states) which then fluoresce.

The rate constants and the mechanisms of these migrations and bimolecular processes are not known. We will attempt to measure these rate constants and to determine the effect of environment on them.

We will investigate rigid glass or oriented crystal solutions of organic molecules in inert or partially inert solvents. [For example: naphalene dissolved in naphthalene-d_8, biphenyl, durene, and E.P.A. (a mixture of ethyl ether, ethyl alcohol, and isopentane)]. The accessibility of the solvents' electron states decreases as we proceed down this series.

Some of the experiments mentioned above had been initiated prior to the start of this project. Measurements of the quantum yields of fluorescence and phosphorescence of naphthalene and a series of halo-naphthalenes have been completed and will be submitted for publication. Preliminary experiments on the determination of the extinction coefficient for triplet-triplet transitions have been completed, but the work will have to be refined before publication. Apparatus is being constructed for the measurement of phosphorescent rise times. Preliminary investigations on the properties and mechanisms of delayed fluorescence are under way.

4.9 Low-Temperature Thermometry

H. H. Plumb, G. Cataland, and M. E. Edlow,
Cryogenics Physics Section

A portion of the National Bureau of Standard's effort in low-temperature thermometry is concerned with the resistance of impurity-doped germanium crystals as a sensitive function of temperature below 20°K. Recently, progress has been made in empirically fitting curves relating resistance and temperature. The results will be published within the next year.

4.10 Oxide Melting-Point Standards

S. J. Schneider,
Crystallography Section

A compilation of the melting points of 70 metal oxides has been published (Schneider, 1963a). Both the original melting point and equivalent value based on the International Practical Temperature Scale of 1948 are presented. Another paper (Schneider, 1963b) clarifies certain misapprehensions about the accepted melting points of corundum, Al_2O_3; magnesium oxide, MgO; calcium oxide, CaO; and chromium sesqui-oxide, Cr_2O_3.

Equipment has been constructed which will permit the heating of samples to 3000°C in a vacuum or inert atmosphere and to 2400°C in an oxidizing environment. Design and testing of black-body enclosures have been adjusted to the aim of achieving the highest attainable accuracy of temperature measurement.

In addition, research is now being conducted on possible reactions between oxides and various container materials such as Ir, Pt, and W. Preliminary information indicates that Ir, in an air environment at 1000°C, oxidizes to IrO_2, which in turn reacts with the various oxides to form binary compounds, At higher temperatures, the compounds dissociate to Ir metal and the original oxide.

4.11 Dilatometric Studies of Polymers

F. A. Quinn, Jr. and J. Powers,
Macromolecules: Synthesis and Structure Section

a) Polybutene-1 undergoes a spontaneous crystal-phase transformation from an initially formed phase with a tetragonal unit cell to a denser rhombohedral one. The crystallization process occurs over the period of a week with a minimum rate at 20°C at atmospheric pressure. Transformation isotherms, over a temperature range of 0°C to 55°C and a pressure range of 1 to 800 kg/cm^2, were measured for polybutene-1 samples in a dilatometry apparatus described by Martin and Mandelkern [J. Appl. Phys., 34, 2312 (1963)].

The transformation rate increases and the temperature at which the maximum rate occurs shifts upward with increasing pressure. In the lower portion of the temperature range, proximity to the glass transition temperature (~ -24°C) undoubtedly influences the transformation process. The presence of a maximum in the rate and its upward shift with temperature (of the same order of magnitude as that of the melting point with pressure) indicate that polybutene-1 recrystallizes through nucleation and growth steps.

b) Polypentene-1 forms at least two polymorphs, a 3_1 and a 4_1 helix, similar to polybutene-1 (NBS Technical Note 174, Section 5.21). The melting point of the 4_1-helical structures is lower (80°C) than that of the 3_1 modification (>100°C). No evidence has been found as yet that the 4_1 helix transforms directly to the 3_1 form as in polybutene-1. Instead, transformation from one to the other seems to require an intervening melt phase. The optimum temperature for this transformation is in the vicinity of 80°C.

4.12 Thermal Conductivity of Paramagnetic Crystals

J. F. Schooley,

Cryogenic Physics Section

During the latter half of 1963, some experimental work has been done on the measurement of the thermal conductivity of neodymium ethylsulfate by the method mentioned in Section 4.9 of NBS Technical Note 197.

Preliminary results indicate a thermal conductivity of the order of 10^{-7} watt (cm deg)$^{-1}$ at 0.04°K, and a variation very nearly as the square of temperature between 0.02°K and 0.05°K.

Measurements on other crystals of neodymium ethylsulfate are contemplated as checks on both the absolute magnitude and the variation with temperature of the conductivity.

4.13 Magnetic-Resonance Studies - I

T. Chang, R. A. Forman, and

R. E. Payne,

Solid State Physics Section

a) Nuclear Resonance

The nuclear resonance of N^{14} in potassium azide, KN_3, has been observed. Information has been obtained on the structure of the N_3^- group and some information on the chemical bonding. Further work is in progress.

Nuclear-resonance experiments on the antiferromagnetic compound $RbMnF_3$ have been completed. Besides a frequency shift of the F resonance similar to that observed in $KMnF_3$ [Shulman and Knox, Phys. Rev., 119, 94 (1960)] shifts of the Rb lines have also been observed. Information on the crystal structure after the phase transition and on the p-d and s-d bonding orbitals have been obtained.

Further studies are in progress on transition-metal oxides and on some

nitrogen compounds which are known to undergo phase transitions.

b) Electron-Spin Resonance

The work on molybdenum-doped rutile, TiO_2, has been completed. The super-hyperfine structure observed in the Mo spectrum indicates that the electron-wave function of Mo spreads out rather far (more than 3 Å) in the host lattice of TiO_2.

The behavior of other ions in TiO_2 is being investigated. Among these is tungsten which shows signs of superhyperfine structure. It is believed that this is the first time that tungsten ESR has ever been observed.

Niobium in strontium titanate, $SrTiO_3$, was examined also. The niobium is probably present in very low concentration and the signal seems to indicate strong saturation.

4.14 Magnetic-Resonance Studies - II

L. M. Matarrese, J. S. Wells, R. L. Peterson,
R. J. Mahler, and A. R. Cook,
Radio and Microwave Materials Section

A yellow-brown specimen of iron-doped synthetic quartz single crystal has been found to give a well-behaved EPR spectrum of ferric ion (Fig. 26) without the extraneous, variable-intensity lines characteristic of the green specimens studied earlier (see NBS Technical Note 197, Section 4.17). So far, our experiments have been carried out only at room temperature in a K-band spectrometer.

Three sets of five lines each are observed, spread out from 4 to 11 kG. The behavior of the sets as the magnet is rotated with respect to the crystal suggests that the ferric ions are distributed amoung three sites differing only in the orientation of their principal axes which are 120° apart in the plane perpendicular to the optic axis (Fig. 27). When the magnetic field is parallel to the optic axis, all three sites give identical spectra which are superposed to give the five lines shown in Figure 26.

From the measurements of line positions as a function of angle of rotation of the magnetic field in the XZ plane of the quartz, we have determined the following values for the spin Hamiltonian: $g_{\parallel}$(along X-axis) = 2.0036, $g_{\perp}$(along optic axis) = 2.0031, D (axial field parameter, assumed positive) = 734.8 G, $|E|$ (rhombic field) = 327.4 G, a_0 (a measure of the cubic field) = 37.7 G. We cannot yet say whether the ferric-ion site is substitutional or interstitial, nor do we yet know how the charge is compensated. Further experiments, including rotations in other planes, are in progress to try to answer these questions and to check the parameters.

A marginal oscillator for the 300 Mc range and associated transmission lines have been built for Electron Nucleus Double Resonance (ENDOR) experiments on single crystals of calcite containing manganese.

The anharmonic creation of nuclear-transition-frequency phonons was observed in sodium chlorate, $NaClO_3$, and reported at the American Physical Society meeting in Edmonton.

We also attempted to observe a nuclear double-spin flip transition between the gallium and arsenic nuclei in single crystals of GaAs but the interaction proved to be too small to be observable.

We have succeeded in producing nuclear-spin transitions of fluorine nuclei via ultrasonic modulation of the magnetic interaction in $KMnF_3$ in the

Fig. 26 EPR spectrum of Fe^{3+} in quartz (synthetic) at K-band and room temperature. Field increases non-linearly from left to right, from about 4500 to 11,300 G. The numbers below the lines indicate the value of M in the transition M⟷M-1, assuming a positive value for D, the axial field-splitting parameter. The lower trace is the H parallel to the Z axis (optic axis) of the quartz. In this orientation, the spectra of all three sites coincide. When the field is parallel to one of the quartz X axes, it is thereby parallel to the principal axis of one of the three sites; the spectrum of this site is labeled by the circled 1's. At the same time, the field makes equal angles (60°) with the axes of the other two sites, whose spectra coincide to give the other five lines observable at this orientation. The origin of the weak lines which can also be seen in these traces is as yet unknown.

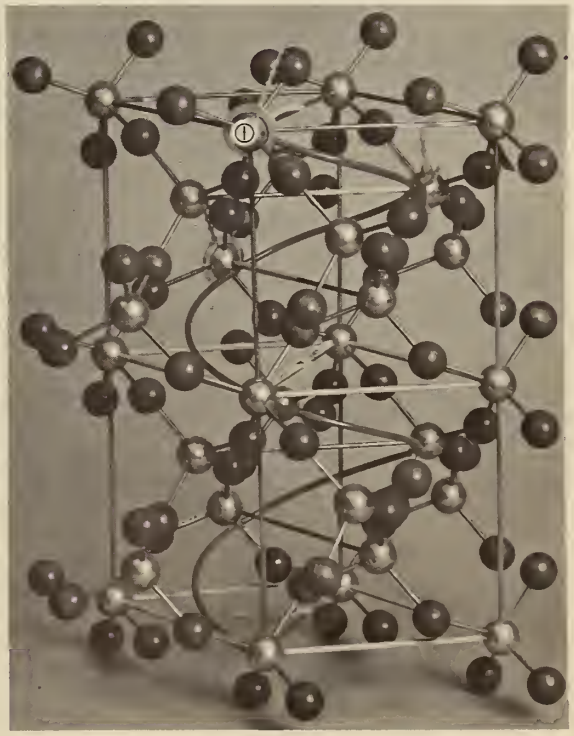

Fig. 27 A model of optically right-handed α-quartz. The optic axis is vertical and is the same as the axis of the left-handed spiral in the model. The three inequivalent substitutional sites are shown near the top of the model and can be identified by the knobby sticks attached to them. Site 1 is labeled; the other two sites are in the layers below it.

antiferromagnetic state. This work is being submitted to Physical Review Letters. At present, we are attempting to observe the ultrasonically modulated magnetic interaction between the aluminum nuclei and the paramagnetic chromium ion in ruby. Success in this experiment will enable us to investigate the nuclear-paramagnetic relaxation process.

4.15 Nuclear-Magnetic-Resonanance Studies in Yttrium-Iron Garnets

R. L. Streever,

Magnetic Measurements Section

The nuclear resonance of Fe^{57} in mixed yttrium-gallium-iron garnets has been studied. Thus far, the resonance has been observed in concentrations where up to forty percent of the iron atoms have been replaced with gallium atoms. These measurements are particularly interesting because nuclear resonance frequency is a measure of the magnetizations on the individual sublattices. The concentration in which this magnetization begins to fall rapidly to zero is of importance in studies of dilute ferromagnetism. It will also be possible to determine the ratio of gallium atoms substituting for iron atoms on "a" and "d" sites. The structure of these crystals, as well as their magnetic properties, is thereby precisely characterized.

4.16 Electron-Spin-Resonance Studies of Transition-Metal Complexes

H. C. Allen and G. F. Kokoszka,

Inorganic Solids Division

The EPR spectrum of the tris-coordination compound of Cu^{+2} with 1-10 phenothroline and 2-2' dipyridine diluted in the matrix of the corresponding zinc compound has been examined as a function of temperature. At high temperatures, a single absorption is observed in each compound indicating an isotropic g-value. At liquid-nitrogen temperature, each compound exhibits an absorption pattern corresponding to an anisotropic g-tensor with two principal values. These spectra have been interpreted as arising from a Jahn-Teller distortion, frozen in at the lower temperatures as described by the theoretical treatment of Liehr and Ballhousen [Ann. Phys., 3, 304 (1958)]. A report on the spectrum of the polycrystalline material was presented at the 144th meeting of the American Chemical Society and has been submitted for publication. Since then, it has been possible to grow some single crystals and work is progressing on these samples.

Crystals of zinc-doped copper acetate monohydrate are being studied by EPR techniques. In the normal crystal the copper ions occur in pairs with an internuclear separation of about 2.6 A. [for reference see Bowers and Owen, Repts. Progr. in Phys., 18, 304 (1955)]. A relatively strong exchange coupling has been observed, and the EPR spectrum is characteristic of a species with a spin of one. By substituting zinc ions into the crystal structure, the behavior of a single copper ion may be studied. The results of this investigation should be submitted for publication early in 1964.

4.17 Low-Temperature Nuclear Orientation

H. Marshak, R. B. Dove, and

R. S. Kaeser,

Cryogenic Physics Section

Helium-3 refrigeration in conjunction with a superconducting split solenoid has been used to obtain a high degree of polarization of a Ho^{165} sample

in the form of a single metal crystal. This target, along with a beam of 350 keV polarized neutrons produced by the Li(p,n) reaction with the Oak Ridge National Laboratory 3MV pulsed Van de Graaff, has enabled us to investigate whether or not a spin-spin interaction exists in the optical model potential. Results of these measurements indicate that the spin-spin interaction, for this particular case, is lower by approximately two orders of magnitude than the spin-orbit interaction. Measurements of the change in total neutron cross-section for an oriented and unoriented deformed nucleus have been made.

4.18 Microwave Measurements on Single-Crystal Ferrimagnetics

A. S. Risley and H. E. Bussey,

Radio and Microwave Materials Section

Small quantities of high-purity single-crystal manganese ferrite and single-crystal yttrium iron garnet were acquired in the past six months. No measurements were made on these materials during this period. Theoretical work coupled with experimental results on ferrimagnetic polycrystals has increased our interest in single-crystal materials. Experimentation on single crystals is planned for the present six-month period.

4.19 Adsorption on Metal Single Crystals

R. Klein,

Surface Chemistry Section

The chemisorption of carbon monoxide on tungsten, observed with a field-emission microscope, showed that the adsorption was non-dissociative. Surface migration and desorption were observed at several temperatures and the activation energies associated with these processes were derived. The specificity of the metal surface is being considered through the study of carbon monoxide adsorption on a variety of metals. Tantalum, for example, shows behavior similar to tungsten in its interaction with carbon monoxide. There are differences in detail related, it may be postulated, to the electronic rather than the geometric structure of the metal. Niobium, as would be expected, is more closely related to tantalum than to tungsten in adsorption of carbon monoxide, CO. It is interesting that the field-emission pattern of tungsten shows the {011}, {001}, and {121} planes as dark areas in the field-emission patterns. These are the areas having relatively high work functions. With tantalum and niobium only the {011} and {001} planes appear as areas of low emission.

The experiments with niobium were done with the field-emission tube immersed in liquid helium. Since the superconducting transition for niobium is 9.2°K, a comparison of patterns and work functions of CO-covered surfaces below and above the transition point was possible. (Temperatures above ambient were achieved by heating a loop wo which the emitter was attached.) No differences could be detected.

It was found for CO on niobium that there are at least three states of adsorption. There is a weakly bound state, present at high coverage, which is desorbed in the 100-200°K range; an intermediate state can be desorbed at 700°K; and the most strongly adsorbed state, present only in a small fraction (perhaps 10^{-2}) of a monolayer, which is desorbed above 1000°K with indication of decomposition of the CO.

The general conclusion is that the chemisorption of CO on clean metal-crystal surfaces is a complex process. No simple model can satisfactorily represent the experimental facts.

4.20 Superconductivity in Niobium

V. D. Arp,

Cryogenic Properties of Solids Section

Superconducting properties of metals depend strongly on the electronic configuration within the metal, and only weakly on the crystalline structure of the metal. An exception to this general rule is that as dislocations are added to the crystal structure, diamagnetism becomes strongly irreversible with applied field. Sensitivity to dislocation content is large in those metals whose Fermi-surface properties give rise to a short electronic-coherence length. Empirical evidence indicates that this coherence length is unusually short in niobium. We have found that available superconductivity theory can predict certain features of the irreversible-magnetization curve of heavily cold-worked niobium (containing perhaps 10^{10} dislocation per cm^2), but that current-carrying capacity in a high field is inconsistent with the theory in this case.

4.21 Experimental Determination of Atomic-Scattering Factors

G. Burley,

Crystallography Section

As the initial step in a program of determining experimental values of the atomic-scattering factors, the determination of an accuracte value for the Debye-Waller temperature exponent for magnesium oxide, MgO, has been undertaken.

Accurate X-ray diffraction patterns have been obtained for several different specimens of polycrystalline MgO, with both copper and molybdenum radiations. The total integrated intensity for each reflection at room temperature has been measured by the pulse-count technique at intervals of 0.05° (2θ). Patterns have also been made with a high-temperature attachment for the diffractometer at 100°C intervals to 400°C. Data reduction is now in progress.

4.22 Soft X-Ray Spectroscopy

R. D. Deslattes,

Crystal Chemistry Section

The vacuum two-crystal spectrometer discussed in NBS Technical Note 197, Section 3.7, was completed by addition of source and detector. It will be described in detail elsewhere. In anticipation of the first planned experiments in the K series of neon and NaF, it was equipped with potassium acid phthalate, KAP, crystals obtained commercially. With these, some exploratory measurements revealed that the KAP crystals exhibited resolving power that was too low to permit serious study of the neon spectrum. It was subsequently demonstrated by means of diffraction topography (see Section 3.13) that the broad rocking curves resulted largely from high dislocation density and severe long-range strain in the samples at hand. Subsequent topographic studies of "specially selected" samples from the commercial source revealed even more strain, larger dislocation density, and bifurcation of the crystal plates. These results have halted the program initially planned. Efforts to produce KAP crystals of adequate perfection for spectroscopy have been initiated by Torgesen, Horton, and Strassburger (see Section 2.8). Seed crystals have been prepared and placed in two baths, one isothermal, and the other temperature programmed. If either or both of these are successful in producing the large specimens required for spectroscopy, then samples should be available for evaluation in the next report period.

Should these exhibit substantially superior characteristics to the samples tested so far, the program can return to its original plan.

In the meanwhile, good specimens of ammonium dihydrogen phosphate, ADP, cut for 101 reflection (2d = 10.6 A) have been obtained (see Sections 2.1 and 2.8). Preliminary spectroscopic results at 8.32 A indicate a resolving power of 10,000. It is planned, therefore, to replace the original program by one involving use of these ADP crystals to study the valence-emission-band structure of some III - V compounds and, where possible, their group IV analogs. These include, in particular, the K spectrum of phosphorus in GaP and the K spectrum of silicon. Also, it is planned to examine in the L series, the valence-emission spectra of germanium, gallium, and arsenic in GaAs.

Completion of these rather extensive plans is dependent on the automation of data acquisition. Components are either on hand or have been ordered at this time.

5. CRYSTAL CHEMISTRY

Contributions to this chapter are concerned with studies of individual crystal phases involving crystal structure, transformations, or chemical properties not sensitively dependnet upon crystal perfection.

5.1 Crystal-Structure Analysis

S. Block, H. M. Ondik, and
A. Perloff,
Crystallography Section

The program of crystal-structure analysis has several facets, including: (a) evaluation of methods of structure analysis, (b) determination of structural principles of inorganic compounds such as borates and phosphates, and (c) compilation of single-crystal data. In recent work certain formulae were tested for applicability and limitations by using them in determining the structure of sodium tetrahydroxyl borate dihydrate, $NaB(OH)_4.2H_2O$ (Block and Perloff, 1963). Other structures determined include 1-ethyldecaborane (Perloff, 1964), sodium trimetaphosphate, $Na_3P_3O_9$, and its hydrate, $Na_3P_3O_9.H_2O$ (Ondik, submitted to Acta Cryst.), and BaB_4O_7 (Block and Perloff, in preparation).

Structural relationships of the low and high temperature forms of lithium phosphate, Li_3PO_4, have been investigated by X-ray powder diffraction and differential thermal analysis (Keffer and Block, in preparation).

5.2 Crystal Chemistry of Calcium Phosphates

W. E. Brown and E. C. Moreno,
Dental Research Section

The sparingly soluble calcium orthophosphates, $CaHPO_4$, $CaHPO_4.2H_2O$, $Ca_8H_2(PO_4)_6.5H_2O$, α-$Ca_3(PO_4)_2$, $\beta.Ca_3(PO_4)_2$, and $Ca_5OH(PO_4)_3$, comprise a group of compounds of considerable commercial and biological importance. Their solubilities in aqueous systems are being measured to gain information that can be used to predict their relative stabilities under the various conditions where they are encountered.

Of these compounds, $Ca_5OH(PO_4)_3$ is of particular significance because it is the prototype for the crystallites in bone and tooth. It bears a

unique structural relationship to the salt $Ca_8H_2(PO_4)_6.5H_2O$, and of major interest is an understanding of how this relationship influences the chemical and crystallographic properties of the two salts. Particular attention is being given to the manner in which $Ca_5OH(PO_4)_3$ may enter into growth mechanisms, solubilities, reaction with fluoride, and incorporation of impurities by the crystallites.

The structure of α-$Ca_3(PO_4)_2$ is being determined from single-crystal X-ray data.

5.3 Standard X-Ray Diffraction Powder Patterns*

H. E. Swanson,

Crystallography Section

Patterns of pure and well characterized inorganic solids are being produced as comparison standards that are used in identifying crystalline materials of unknown composition. These patterns have been published in twelve volumes. A thirteenth (Swanson et al., 1964) includes patterns for 51 substances, thirty of which were not previously included in the X-ray Powder Data File issued by the Joint Committee on Chemical Analysis by X-Ray Diffraction. Twenty-one are to replace earlier and less reliable patterns based on various sources.

A computer is being used to calculate powder-pattern intensities and spacings from single-crystal data in the case of materials for which observed data are difficult to obtain.

5.4 Crystals with Large Lattice Spacings

H. E. Swanson,

Crystallography Section

In a search for crystals with large-lattice spacings suitable for use in long wavelength X-ray spectroscopy, X-ray powder diffraction patterns for eighteen organic samples (supplied by Leo A. Wall, Polymer Chemistry Section) and for a number of metal biphthalates prepared in this laboratory were examined. In each group, one or more compounds were found that have strong reflections at low angles and are worthy of further consideration.

5.5 Phase Equilibria

E. M. Levin and R. S. Roth,

Crystallography Section

Phase-equilibria research is conducted in three areas: (a) glass-forming systems containing silica, germania, and boric oxide; (b) systems of interest in electronic research, such as those containing niobia, tantala, and zirconia; and (c) refractory oxide systems, in particular, those containing rare-earth oxides.

---

* This work is partially supported by the Joint Committee on Chemical Analysis by X-Ray Diffraction under the auspices of the American Society for Testing and Materials, the American Crystallographic Association, the British Institute of Physics, and the National Association of Corrosion Engineers.

In a two-part paper on the polymorphism of bismuth sesquioxide, Bi_2O_3, (Levin and Roth, 1963) discrepancies in the literature have been resolved and, in addition, the effects of oxide additions on the polymorphism of this compound have been reported for 33 selected oxides.

The solid solution reported to occur in niobia for small cation additions has been shown actually to consist of discrete phases, apparently isostructural with the mixed tantalum niobium oxide of formula $Ta_2O_5.2Nb_2O_5$ (Waring and Roth, 1963). The crystal structures of members of this series are being studied by Roth in collaboration with A. D. Wadsley in Australia.

Results of a study of the stability of bismuth- and stibio-tantalites have been reported (Roth and Waring, 1963).

5.6 Allotropy in Some Rare-Earth Metals at High Pressures

G. J. Piermarini and C. E. Weir,
Crystallography Section

Work on the lattice parameters and energies of the high-pressure polymorphs of some alkali halides (NBS Technical Note 197, Section 5.6) has been completed (Weir and Piermarini, 1964a).

Most of the rare-earth metals have been obtained and are now being studied. Using an X-ray diffraction camera which incorporates a diamond-anvil high-pressure cell, studies have been completed on lanthanum, cerium, praseodymium, and neodymium up to 60 kilobars (Piermarini and Weir, 1964b). These studies show that for each of these metals a high-pressure modification exists which has a face-centered cubic structure. Cerium was observed to undergo an electronic transition from an fcc to a "collapsed" fcc structure, corroborating previously published results. Apparently, the structural nature of the transitions in lanthanum, praseodymium, and neodymium (hcp to fcc) has never been reported.

5.7 Crystal Chemistry of Silver Iodide*

G. Burley,
Crystallography Section

The general survey of solid-state properties of silver iodide has been continued (compare NBS Technical Note 197, Section 5.11). The Debye temperature, strain distribution, and atomic arrangements near the β-α transition temperature have been studied and some paramagnetic-resonance data from the literature have been evaluated in terms of other behavior. The Debye temperature was evaluated both from the change of integrated intensities of a single X-ray reflection over the range from 20° to 120°K for the cubic phase, and from the variation of intensities with Bragg angle at room temperature for a single crystal of the hexagonal phase. These techniques gave values of 116° and 119°K, respectively, compared with 116°K from heat-capacity data and 107°K from elastic-moduli determined at room temperature.

Line-broadening analysis of finely ground polycrystalline silver iodide compared with carefully annealed specimens indicated that the entire contribution to the difference of intrinsic breadth was due to strain and,

---

* Research supported by the Atmospheric Sciences Program, National Science Foundation.

essentially, not to the effects of small domain size. The strain is nearly isotropic, with an average value of $\Delta d/d = 4.4 \times 10^{-3}$ and the calculated stored elastic energy is 0.66 cal g^{-1}. Because of the absence of higher-order reflections, analytical methods rather than the more precise Fourier analysis of peak shapes had to be used.

The previous observation that ice crystals nucleated by freshly prepared silver iodide smoke had a hexagonal habit, while those formed after exposing the nuclei to strong light had a rectangular habit has been tentatively explained. The change appears due to the differential rates of photolytic disordering on the prism and basal surfaces of silver iodide. The rate of ice nucleation has been postulated elsewhere [Mason, Phil. Mag., 8, 505 (1963)] to depend on the migration distance of surface atoms, so that growth is slowest on those surfaces allowing maximum movement. The preferential destruction of trapping sites on the prism faces during the initial stages of irradiation is then postulated to account for the observed change of habit.

A radial-distribution analysis of X-ray powder-diffraction patterns from the low-cubic and hexagonal phases just above the transition of both to the high-cubic phase has revealed substantial differences in bonding. An analysis of these in terms of specific-site occupation statistics is now in progress.

Studies of polymorphism (Burley, 1963a) and of primary X-ray extinction of polycrystalline samples exposed to light (Burley, 1963b) as well as lattice-mode analysis of the thermal-expansion behavior (Bienenstock and Burley, 1963) have now been published.

5.8 Rapid X-Ray Diffraction Photography of Polycrystalline Materials

R. E. LaVilla,
Crystal Chemistry Section

A miniature focusing camera has been fabricated and tested in conjunction with a microfocus X-ray generator. From a 0.005 in.-thick copper shim-stock specimen, a good powder pattern was obtained on X-ray film, with an exposure (at 50 kV and 2.5 mA) of about 0.2 seconds and with unfiltered copper radiation from a 100-micron spot.

Present plans are to complete the installation of an electronic image intensifier and to investigate the possibility of controlling the exposure time by electronically pulsing the grid of an X-ray cathode gun. The possible fabrication of a very high intensity pulsed X-ray tube with a disposable target is also under study.

5.9 Structure of Silica Whiskers

H. C. Duecker and W. K. Haller,
Glass Section

The silica whiskers previously described (NBS Technical Note 197, Section 5.13) can be grown in a manner which yields a modification of silica unlike any known previously. The monochromatic X-ray diffraction pattern obtained from the finely ground whiskers is similar to that reported for vitreous silica except that several additional humps appear in the curve. The radial-distribution curve calculated with the Debye scattering equation and the method of Warren indicates interatomic distances corresponding to those found in a pentagonal $(Si\text{-}O)_5$ ring. The calculated X-ray diffraction curve for this ring model in turn has maxima corresponding to the humps found in

the experimental X-ray diffraction curve. Since the whiskers used in the X-ray studies were known to be homogeneous (on the basis of refractive index and density) the whiskers may be looked upon as partially ordered vitreous silica.

5.10 Structure Models for Amorphous and Crystalline Phases of Simple Substances

F. Ordway,

Inorganic Solids Division

A random network of 300 tetrahedral units has been constructed and measurements have been made for the determination of all coordinates. A ring-counting routine has been written for the IBM 7090 computer and used with the topological data for the model to tabulate the distribution of ring sizes. Routines for processing the geometrical data are being prepared. A paper on this work was presented at the Sixth Congress of the International Union of Crystallography in Rome, September, 1963.

5.11 Radial-Distribution Studies of Glasses

S. Block and G. J. Piermarini,

Crystallography Section

In connection with a study of immiscibility, models were proposed for the cation-modifier distribution in borate and silicate glasses. On the basis of these models certain interatomic vectors are expected. X-ray diffraction studies have been used to obtain independent information about these interatomic vectors. In the past several months, radial-distribution studies of strontium borate glasses, in conjunction with previous studies on barium- and cadmium-containing glasses (Block, Molin, and Piermarini, 1963) have indicated a similarity of cation distribution in all these systems. This short-range order is similar to that found in crystalline barium diborate, $BaO.2B_2O_3$, whose structure has been determined in this laboratory. Future work is planned to explore the limitations of the similarity of cation distribution in the vitreous and crystalline states.

5.12 High-Resolution Small-Angle X-Ray Camera

H. Brumberger,

Crystal Cehmistry Section

A small-angle scattering camera, employing the Borrmann effect in germanium for collimation (see NBS Technical Note 197, Section 5.5) was assembled.

Test exposures of the scattering from carbon indicate that spacings as large as about 2000 Å are resolved.

A brief note giving details regarding the instrument has been prepared and will be submitted for publication.

5.13 Physical Structure of Crystalline Copolymers

R. K. Eby,
Polymer Physics Section, and
L. H. Bolz,
Physical Properties Section

Electron microscopy and small-angle X-ray diffraction show copolymers of tetrafluoroethylene and hexafluoropropylene to be lamellar. Consideration of lamellar thickness (typically 200 to 500 Å) together with the concentration of perfluoromethyl groups indicates that the groups are incorporated in the crystalline lamellae and therefore occur as point defects in the lattice (Eby, 1963 and 1964). The increase of lattice parameters which should accompany the presence of these point defects has been observed in diffraction patterns obtained with a powder camera at 23°C (Eby, 1964). However, this result is subject to some question because the weak diffraction at large angles makes correction for film shrinkage difficult. There is also another question arising from the fact that polytetrafluoroethylene undergoes first-order transitions at about 290 and 305°K. These transitions, at which both the lattice parameters and the thermal coefficients of expansion increase, occur at lower temperatures in the copolymers [McCrum, Makromol. Chemie, 34, 50 (1959)]. Thus, it can be asked whether the lattice of the copolymer is larger than that of polytetrafluoroethylene at 23°C, merely because the copolymer is at a higher temperature with respect to the phase transitions. For these reasons, more accurate measurements have been made over a lower temperature range with a diffractometer, a cold cell (Block et al., 1958) and an "internal" standard of silicon. A thin layer of the standard was placed on the front surface of the samples and used, together with previous measurements of silicon (Mauer and Bolz 1955) and [Novika and Strelkov, Soviet Phys., Solid State, 1, 1687 (1960)] to keep the diffractometer adjusted. The data show the lattice of the copolymer to be larger than that of polytetrafluoroethylene, even below the transition temperature, which is near 225°K for a copolymer with about six perfluoromethyl groups per hundred main-chain carbon atoms.

5.14 High-Pressure Microscopy of Crystal Transformation and Growth

A. Van Valkenberg,
Crystallography Section

Earlier work on the high-pressure microscopy of the silver and cuprous halides (NBS Technical Note 197, Section 5.9) has been published (Van Valkenburg, 1964).

The triple point of ice VI, ice VII, and liquid water has been observed under the microscope at a pressure of 22.4 kilobars and a temperature of 80° C. At the triple point, skeletal crystals of ice VI and VII can be observed forming and melting in the liquid phase with considerable activity. The triple point has been approached by three independent routes following the boundary lines between (1) ice VI and liquid, (2) ice VI and ice VII, and (3) ice VII and liquid. It was observed that the birefringence of ice VI decreases as the triple point is approached. It was also observed that the refractive indices of ice VI approached that of the liquid phase as the triple point is approached. The sensitivity of this triple point to slight changes of pressure or temperature is very high and it should make a good reference point.

Using a gasketing technique with the diamond cell, we observed optical changes in single crystals or crystal fragments (.2 mm in length) at hydrostatic pressures up to 30 kilobars and a temperature of 150°C. Kerosene is

one of the liquids used to obtain hydrostatic conditions at a pressure of approximately 15-20 kilobars. It was observed that kerosene changes to a mush of crystallites and liquid above 10 kilobars. The crystallites appear to have a low birefringence and the liquid is somewhat viscous.

Calcium carbonate has two reversible transitions, one at 14 kilobars and the other at 17 kilobars at room temperature. These two transitions were observed in single-crystal fragments under hydrostatic conditions with temperature changes of up to 100°C. The transition at 14 kilobars was observed as a barely perceptible wave crossing the crystal fragment. This transition is interpreted as being a slight change in the symmetry of the crystal similar to the α-β transition in quartz. The second transition at 17 kilobars has a volume change of 2.7% according to Bridgman and this transition can readily be observed as a sluggish wave front passing from one end of the crystal to the other. The crystal changes from one having a uniform birefringence to one of distorted birefringence, suggesting a change from an ordered to a disordered structure. When pressure is released there is a reverse transition and the birefringence becomes uniform.

5.15 Optical Observations of Pressure-Induced Transformation in Polymers

J. Powers,

Macromolecules: Synthesis and Structure Section

Light-transmission measurements previously reported (NBS Technical Note 197, Section 5.8) were continued. The transmission of the diamond anvils with no sample between them has been measured. The transmission of natural rubber has been determined. The resulting curve does not show the abrupt transmission increase over a narrow pressure range exhibited by Teflon and several other semi-crystalline polymers. Ancillary studies using density-gradient tubes on the effect of compression upon polymer density have been started.

5.16 Infrared Spectroscopy of Crystalline Inorganic Borates

C. E. Weir and R. A. Schroeder,

Crystallography Section

Plans for this work were announced in NBS Technical Note 197, Section 5.7. Infrared spectra have been obtained on a large number of crystalline inorganic borates at room temperature. The data have been compiled and the results are being prepared for publication.

At the present time, it can be concluded that the spectra of most orthoborates and pyroborates can be interpreted in terms of vibrations of the BO_3 and B_2O_5 groups, respectively, and consistent assignments of the observed bands can be made. For some metaborates a satisfactory assignment of the spectra can also be given, but the borates having anions with ring structures generally show spectra of such complexity that even a superficial interpretation is not possible. From correlations between spectra and structure it is believed that both 3-fold and 4-fold coordinated boron can be identified with reasonable assurance on the basis of the infrared-absorption spectrum alone. Very good correlations between structure and spectra have been observed in many instances.

5.17 Crystal-Field Studies by Matrix Spectroscopy

D. E. Mann,

Molecular Spectroscopy Section

The investigation of crystal-field effects through their influence on the infrared spectra of hydrogen and deuterium-halide molecules isolated in argon and other matrices at low temperatures has been carried to an advanced stage. The vibration-rotation spectrum of HCl in argon in the range 4-20°K has served as the basis of a theoretical analysis recently published by Flygare [J. Chem. Phys., 39, 2263 (1963)] in which it is shown that for an octahedral site the major effect is that due to the interaction of a permanent molecular hexadecapole charge distribution with the fourth gradient of the electric potential at the molecular center of mass. The results for DCl however, indicate that the theory does not yet adequately account for the interaction of the center of mass motion with molecular rotation, and remains to be further developed. However, the main features of the HCl spectra are accounted for.

The non-rotating features in the spectra have been subjected to very intensive investigation during the past year. In particular, the widths and positions of the so-called Q lines for HCl in argon and krypton have been measured with very high resolving power over a considerable temperature range — up to 51°K in krypton. It was found that the lines are remarkably narrow, their width being of the order of 0.15 - 0.25 cm^{-1}, and that both the widths and line positions show a small but definite temperature dependence. Moreover, it was discovered after a long series of careful measurements that initial conditions — deposition rate, concentration, substrate, and impurities — have a pronounced effect on the proportion of rotating to non-rotating features in the spectra. Now that these factors have been sorted out, the influence of the nature of the site, the phase, and indeed the crystallization process itself can come under detailed study with the assistance of the molecular spectrum as an indicator.

5.18 Spectroscopy of Diatomic Impurities in Rare-Gas Crystalline Matrices

G. L. Pollack,

Crystal Chemistry Section

The effect of impurities on crystal growth and the mechanism of zone refining for molecular crystals at low temperatures have been studied by examining absorption spectra of diatomic species in argon and krypton (Pollack, 1964). The experiments are also of spectroscopic interest. Some transitions have been observed which may be due to charge exchange in the solution lattices, or to perturbation of energy levels in otherwise forbidden transitions so that they are allowed.

5.19 Molecular Energy Levels

S. Abramowitz,

Heat Division

A study of the infrared absorption spectra of carbon monoxide, CO, and methane, CH_4, in condensed phases of oxygen, nitrogen, and argon has been made.

The ν_3 fundamental of CH_4 was found at 3017 cm^{-1} in an oxygen solution with a half width of 18cm^{-1}. The position and half width in liquid oxygen were the same at 90°, 78°, and 55°K. In liquid nitrogen at 78°K, the ν_3 vibration was located at 3016 cm^{-1}, and in liquid argon at about 80°K at

3018 cm^{-1}, with half widths of 17 and 23cm^{-1}, respectively. In a clear crystalline argon solid the peak was located at 3023 cm^{-1} with a half width of 25cm^{-1}. This was the only system in which a blue shift relative to the Q branch maximum vapor frequency of 3019 cm^{-1} was observed.

Infrared absorption spectra of CO in the region of the first overtone have been observed in dilute (approximately 1 to 10 parts in 1000) liquid solutions of oxygen, nitrogen, and argon, and clear crystalline nitrogen and argon matrices. The overtone band was found at 4249.0, 4252.4, and 4252.0 cm^{-1} with half widths of 18.4, 17.8, and 13.7cm^{-1} in liquid oxygen, nitrogen, and argon solutions at 82°K and 78°K, respectively. The half width in liquid oxygen varied from 18.4 to 10.0cm^{-1} in the temperature range 82°K to 57°K. The band position was the same but its width was smaller in the crystalline nitrogen matrix. Two bands were observed in the clear crystalline argon solid at 4245 and 4256 cm^{-1}. The solution results cannot be interpreted with the recent theory of Buckingham, nor can the temperature dependence of the half width observed in liquid oxygen be explained with existing models.

The work on methane has been published by Abramowitz and Broida (1963).

6. PARTIAL LIST OF PARTICIPANTS

There follows a partial list of scientists engaged in activities described in this note, with indications of their research fields and organizational location within the National Bureau of Standards. The latter may be helpful in making contact with individuals for the purpose of obtaining reprints or further technical information.

Participants at the Washington Laboratories:

Abramowitz, Stanley: Ph.D. Polytechnic Institute of Brooklyn, 1963; infrared molecular spectra; Heat Division. Author: 5.19

Allen, Harry C., Jr.: Ph.D. University of Washington, 1951; electron-spin-resonance studies; Chief, Inorganic Solids Division. Author: 4.16

Ambler, Ernest: Ph.D. Oxford University England, 1953; nuclear reactions, low-temperature magnetism; Chief, Cryogenic Physics Section, Heat Division.

Anderson, Richard L.: Growth and evaporation of whiskers; Cryogenic Physics Section, Heat Division. Author: 2.21

Barber, David J.: Ph.D. University of Bristol, England, 1959; growth perfection of crystals; Physical Properties Section, Inorganic Solids Division. Author: 3.4

Bass, Arnold M.: Ph.D. Duke University, 1949; molecular spectroscopy; Heat Division.

Becker, James H.: Ph.D. Cornell University, 1957; optical and transport properties of semiconductors; Solid State Physics Section, Atomic Physics Division. Author: 4.4

Block, Stanley: Ph.D. Johns Hopkins University, 1955; X-ray crystallography; Crystallography Section, Inorganic Solids Division. Author: 5.1;5.11

Blunt, Robert F.: Ph.D. Rice University, 1949; optical properties of solids; Solid State Physics Section, Atomic Physics Division. Author: 3.2

Bolz, Leonard H.: Crystal perfection by electron microscopy; Physical Properties Section, Inorganic Solids Division. Author: 5.13

Bowman, Horace A.: Cartesian diver; Mass and Volume Section, Metrology Division.

Breen, David E.: Inter- and intramolecular properties of organic molecules, crystals, and rigid glasses; Physical Chemistry Division. Author: 4.8

Brower, William S.: Crystal growth by Verneuil process and floating-zone technique; Crystal Chemistry Section, Inorganic Solids Division. Author: 2.5

Brown, Walter E.: Ph.D. Harvard University, 1949; solubility and crystallography of calcium phosphate; Dental Research Section, Polymers Division. Author: 5.2

Brumberger, Harry: Ph.D. Brooklyn Polytechnic Institute, 1955; low-angle X-ray scattering, critical phenomena, and structure of liquids; present address: Chemistry Dept., Syracuse University. Author: 5.12

Burley, Gordon: Ph.D. Georgetown University, 1962; crystallography of silver iodide; Crystallography Section, Inorganic Solids Division. Author: 4.21;5.7

Calvert, Joan P.: Growth of oxide films; Corrosion Section, Metallurgy Division.

Cataland, George: Low-temperature thermometry; Cryogenic Physics Section, Heat Division. Author: 4.9

Chang Te-Tse: Ph.D. University of Colorado, 1962; magnetic resonance; Solid State Physics Section, Atomic Physics Division. Author: 4.13

Cohen, Martin I.: X-ray Diffraction studies of crystals grown at high temperatures; Solid State Physics Section, Atomic Physics Division. Author: 3.15;3.19

Cook Richard K.: Ph.D. University of Illinois, 1935; acoustics and solid state physics; Chief, Sound Section, Mechanics Division.

Cooter, Irvin L.: Nuclear magnetic resonance in garnets; Chief, Magnetic Measurement Section, Electricity Division.

Coriell, Sam R.: Ph.D. Ohio State University, 1961; mathematical physics; Cyrstallization of Metals Section, Metallurgy Division. Author: 2.4

Crissman, John M.: Ph.D. Pennsylvania State University, 1963; polymer physics; Postdoctoral Fellow, Polymer Physics Section, Polymers Division. Author: 2.11

deKoranyi, Alexandra: Crystal growth by electrodeposition, Electrolysis and Metal Deposition Section, Metallurgy Division. Author: 3.10

Deslattes, Richard D.: Ph.D. Johns Hopkins University, 1959; X-ray spectroscopy; Crystal Chemistry Section, Inorganic Solids Division. Author: 3.13;4.22

deWit, Roland: Ph.D. University of Illinois, 1959; dislocation theory; Lattice Defects and Microstructures Section, Metallurgy Division. Author: 2.3; 3.9

Dickson, Robert W.: Homogeneous stress on oxide structures; dislocation studies by X-ray methods; Physical Properties Section, Inorganic Solids Division. Author: 2.1; 4.1

Dove, Robert B.: Nuclear magnetism; Cryogenic Physics Section, Heat Division. Author: 4.17

Duecker, Heyman C.: Physical chemistry of glasses; Glass Section, Inorganic Solids Division. Author: 5.9

Early, James G.: Ph.D. Rennsalaer Polytechnic Institute, 1963; kinetics of crystallization; Crystallization of Metals Section, Metallurgy Division. Author: 2.2

Eby, Ronald K.: Ph.D. Brown University, 1958; acoustics, polymer physics; Polymer Physics Section, Polymers Division. Author: 5.13

Edlow Martin E.: Low-temperature thermometry; Cryogenic Physics Section, Heat Division. Author: 4.9

Eisenstein, Julian C.: Ph.D. Harvard University, 1948; low-temperature magnetism; Cryogenic Physics Section, Heat Division.

Escalante, Edward: Field emission; Corrosion Section, Metallurgy Division. Author: 2.24

Evans, Eloise H.: Physical chemistry, X-ray diffraction; Crystallography Section, Inorganic Solids Division, A.S.T.M. Fellowship supported.

Farabaugh, Edward N.: Etch-pits crystal orientation; Crystal Chemistry Section, Inorganic Solids Division. Author: 2.5

Foley, Carol L.: Growth of oxide films; Corrosion Section, Metallurgy Division. Author: 3.5

Forman, Richard A.: Nuclear and quadrupole resonance; Solid State Physics Section, Atomic Physics Division. Author: 4.13

Franklin, Alan D.: Ph.D. Princeton University, 1949; properties of point defects in crystals; c/o Inorganic Solids Division.

Frederikse, Hans P. R.: Ph.D. Leiden University, the Netherlands, 1950; semiconductors at low temperatures; Chief, Solid State Physics Section, Atomic Physics Division. Author: 4.4

French, Judson C.: Solid state divices and materials; Electron Devices Section, Instrumentation Division. Author: 3.12

Frolen, Lois J.: Ph.D. Pennsylvania State University, 1963; spectroscopy, crystallography, microscopy; Analytical Chemistry Division. Author: 2.9,2.10;3.17

Glasgow, Augustus R.: D. Sc. University of Brussels, 1957; preparation and purification of polymeric forms, phase equilibria, purity determinations at high pressures; Analytical and Purification Section, Analytical Chemistry Division.

Gornick Fred: Ph.D. University of Pennsylvania, 1959; physical chemistry of high polymers; Polymers Division. Author: 2.10

Grabner, Ludwig H.: Ph.D. Columbia University, 1950; semiconductors, photoconductivity,; Solid State Physics Section, Atomic Physics Division. Author: 3.18

Greenspan, Martin: Ultrasonics, mechanics; Sound Section, Mechanics Division.

Haller Wolfgang K.: Ph.D. University of Vienna, 1950; physical chemistry of glasses; Glass Section, Inorganic Solids Division. Author: 5.9

Hardy Stephen C.: Vapor growth of metal crystals; Crystallization of Metals Section, Metallurgy Division. Author: 2.21; 2.23

Harman, George G.: Solid state physics, surface phenomena and electroluminescence; Electron Devices Section, Instrumentation Division. Author: 3.12

Hoffman, John D.: Ph.D. Princeton University, 1949; dielectrics, nucleation rate of polymer crystals; Chief, Polymers Division. Author: 2.13

Horton, Avery T.: Crystal growth, impurity retention; Crystal Chemistry Section, Inorganic Solids Division. Author: 2.8

Hosler, William R.: Electronic transport phenomena; Solid State Physics Section, Atomic Physics Division. Author: 4.4

Howard, Robert E.: Ph.D. Oxford University, England, 1957; theoretical physics; Chief, Metal Physics Section, Metallurgy Division. Author: 2.3; 2.22

Hudson, Ralph P.: Ph.D. Oxford University, England, 1949; low-temperature magnetism; Chief, Heat Division. Author: 3.1

Ives, Lewis K.: Electron microscopy; Lattice Defects and Microstructures Section, Metallurgy Division. Author: 2.19

Kaeser, Robert S.: Low-temperature magnetism, cryogenics; Cryogenic Physics Section, Heat Division. Author: 4.17

Kahn, Arnold H.: Ph.D. University of California, 1955; band structure of rutile crystals, paramagnetic impurities in rutile crystals; Solid State Physics Section, Atomic Physics Division. Author: 4.3

Keezer, Richard C.: Optical properties and physical chemistry of semiconductors; Solid State Physics Section, Atomic Physics Division. Author: 3.18

Keller, Richard A.: Ph.D. University of California, 1961; inter- and intramolecular properties of organic molecules, crystals, and rigid glasses; Physical Chemistry Division. Author: 4.8

Khoury, Fred: Ph.D. Leeds University, 1956; morphology and crystallization of polymers; Polymer Physics Section, Polymers Division. Author: 2.14

Klein, Ralph: Ph.D. University of Pittsburg, 1950; field-emission and low-temperature chemistry; Chief, Surface Chemistry Section, Physical Chemistry Division. Author: 4.19

Kokoszka, Gerald F.: Electron-spin-resonance studies; Inorganic Solids Division. Author: 4.16

Kruger, Jerome: Ph.D. University of Virginia, 1953; corrosion reactions at metal surfaces; Corrosion Section, Metallurgy Division. Author: 3.5

LaVilla, Robert E.: Ph.D. Cornell University, 1960; study of transient phenomena by diffraction techniques; Crystal Chemistry Section, Inorganic Solids Division. Author: 5.8

Levin, Ernest M.: Phase equilibria of oxide systems; Crystallography Section, Inorganic Solids Division. Author: 5.5

Lippincott, Ellis R.: Ph.D. Johns Hopkins University, 1947; infrared spectroscopy; Crystallography Section, Inorganic Solids Division.

Mangum, Billy W.: Ph.D. University of Chicago, 1961; low-temperature magnetism; Cryogenic Physics Section, Heat Division. Author: 3.1

Mann, David E.: Ph.D. University of Chicago, 1948; spectroscopy; Chief, Molecular Spectroscopy Section, Physical Chemistry Division. Author: 5.17

Margoshes, Marvin: Ph.D. Iowa State University, 1953; spectrographic analysis; Spectrochemical Analysis Section, Analytical Chemistry Division. Author: 3.3

Marshak, Harvey: Ph.D. Duke University, 1955; nuclear reactions, cryogenics; Cryogenic Physics Section, Heat Division. Author: 4.17

Marvin Robert S.: Ph.D. University of Wisconsin, 1949; rheology and polymer physics; Chief, Rheology Section, Mechanics Division.

Mauer, Floyd A.: Instrumentation for crystallography; Crystallography Section, Inorganic Solids Division. Author: 3.14

McMurdie, Howard F.: Crystallography and chemical phase studies; Chief, Crystallography Section, Inorganic Solids Division.

McNish, Alvin G.: Precise density determinations for solid materials; Chief, Metrology Division.

Miller, Paul R.: High-temperature crystal growth, crystal orientation; Crystal Chemistry Section, Inorganic Solids Division. Author: 2.6

Milligan, Dolphus E.: Ph.D. University of California, 1958; molecular spectroscopy; Molecular Spectroscopy Section, Physical Chemistry Division.

Moreno, Edgard C.: Ph.D. University of California, 1957; physical chemistry; Dental Research Section, Polymers Division. Author: 5.2

Morris, Marlene C.: Physical chemistry, X-ray diffraction; Crystallography Section, Inorganic Solids Division, A.S.T.M. Fellowship supported.

Ogburn, Fielding: Electrochemistry, electrodeposition; Electrolysis and Metal Deposition Section, Metallurgy Division. Author: 2.16;2.17;3.10

Ondik, Helen M.: Ph.D. Johns Hopkins University, 1957; crystallography, inorganic chemistry; Crystallography Section, Inorganic Solids Division. Author: 5.1

Ordway, Fred: Ph.D. California Institute of Technology, 1949; X-ray crystallography; Inorganic Solids Division. Author: 2.6;5.10

Orem, Theodore H.: Mechanisms of corrosion processes; Corrosion Section, Metallurgy Division. Author: 2.1;3.11

Oser, Hans J.: Ph.D. University of Freiburg, 1957; boundary value problems; Applied Mathematics Division. Author: 2.22

Paretzkin, Boris: Study of perfection of single crystlas by X-ray diffraction; Crystal Chemistry Section, Inorganic Solids Division. Author: 2.17;3.16

Parker, Robert L.: Ph.D. University of Maryland, 1960; growth of crystals; Chief, Crystallization of Metals Section, Metallurgy Division. Author: 2.1;2.2;2.4;2.21;2.22;2.23

Passaglia, Elio: Ph.D. University of Pennsylvania, 1955; mechanical relaxation processes in polymers; Polymer Physics Division. Author: 2.11

Payne, Richard E.: Nuclear resonance; Solid State Physics Section, Atomic Physics Division. Author: 4.13

Peiser, H. Steffen: Crystallography and crystal chemistry; Chief, Crystal Chemistry Section, Inorganic Solids Division. Author: 2.17;3.7;3.16

Perloff, Alvin: Structure analysis; Crystallography Section, Inorganic Solids Division. Author: 5.1

Pfeiffer, Earl R.: Crystal growth from solution; Cryogenic Physics Section, Heat Division.

Piermarini, Gasper J.: Radial-distribution studies; high-pressure X-ray diffraction studies; Crystallography Section, Inorganic Solids Division. Author: 5.6;5.11

Plumb, Harmon H.: Ph.D. Northwestern University, 1954; low-temperature thermometry; Cryogenic Physics Section, Heat Division. Author: 4.9

Pollack, Gerald L.: Ph.D. California Institute of Technology, 1962; low-temperature physics; Crystal Chemistry Section, Inorganic Solids Division. Author: 2.18;5.18

Pontius Paul E.: Accurate measurements of mass, volume, and density; Chief, Mass and Volume Section, Metrology Division.

Powers, Joseph: Ph.D. University of Massachusetts, 1961; kinetics, morphology, and mechanism of crystallization of polymers; Macromolecules: Synthesis and Structure Section, Polymers Division. Author: 2.15;4.11;5.15

Proctor, Thomas M.: Solid state physics; Sound Section, Mechanics Division.

Quinn, Fred A.: Crystallization rate of high polymers; Macromolecules: Synthesis and Structure Section, Polymers Division. Author: 4.11
Rasberry, Stanley D.: Spectrographic analysis; Spectrochemical Analysis Section, Analytical Chemistry Division. Author: 3.3
Read, Susan F.J.: Ph.D. Oxford University, England, 1963; solid state physics; Temperature Physics Section, Heat Division.
Robbins, Carl R.: Phase-rule equilibria of inorganic systems; Crystallography Section, Inorganic Solids Division.
Roberts, D. Ellis: Crystal growth; Solid State Physics Section, Atomic Physics Division. Author: 2.7
Robinson, Henry E.: Thermal conductivity measurement on solids at high and low temperatures; Chief, Heat Transfer Section, Building Research Division.
Ross, Gaylon S.: Nucleation, crystal growth; Analytical Chemistry Division. Author: 2.9;2.10;3.17
Roth, Robert S.: Ph.D. University of Illinois, 1951; X-ray diffraction studies, phase equilibria; Crystallography Section, Inorganic Solids Division. Author: 5.5
Rubin, Robert J.: Ph.D. Cornell University, 1951; theoretical chemical physics; Heat Division.
Rubin, Sherwin: Electronic engineering; Engineering Electronics Section, Instrumentation Division. Author: 4.5
Ruff, Arthur W.: Ph.D. University of Maryland, 1963; dislocations and etch pits; Chief, Lattice Defects and Microstructures Section, Metallurgy Division. Author: 2.19;3.8
Ruthberg, Stanley: Materials and physics of vacuum devices; Electron Devices Section, Instrumentation Division.
Saylor, Charles P.: Ph.D. Cornell University, 1928; precise characteristics of compounds, accurate microscopic measurements of optical properties; Analytical Chemistry Division.
Schafft, Harry A.: Semiconductor devices and breakdown phenomena; Electron Devices Section, Instrumentation Division. Author: 3.12
Schneider, Samuel J.: Phase equilibria of oxide systems and melting-point standards; Crystallography Section, Inorganic Solids Division. Author: 4.10
Schooley, James F.: Ph.D. University of California, 1961; crystal growth for low-temperature paramagnetic studies; Cryogenic Physics Section, Heat Division. Author: 4.12
Schoonover, Irl C.: Ph.D. Princeton University, 1933; research administration, NBS Deputy Director.
Schroeder, Rudolph A.: Ph.D. University of Maryland, 1957; infrared spectroscopy; Crystallography Section, Inorganic Solids Division. Author: 5.16
Scribner, Bourdon F.: Analytical applications of optical and X-ray spectroscopy; Chief, Spectrochemical Analysis Section, Analytical Chemistry Division. Author: 3.3
Simmons, John A.: Ph.D. University of California, 1961; mathematical physics; Metal Physics Section, Metallurgy Division. Author: 2.22
Spinner, Sam: Elastic properties of inorganic solids; Physical Properties Section, Inorganic Solids Division. Author: 3.6;4.1
Streever, Ralph L.: Ph.D. Rutgers University, 1960; nuclear magnetic resonance; Magnetic Measurements Section, Electricity Division. Author: 4.15
Swanson, Howard E.: Physical chemistry, X-ray diffraction; Crystallography Section, Inorganic Solids Division. Author: 5.3;5.4
Swartzendruber, Lydon J.: Solid state physics; Electron Devices Section, Instrumentation Division. Author: 3.12
Termini, Dominic J.: Nucleation and crystal growth; Analytical Chemistry Division. Author: 2.10
Thurber, Willis R.: Thermoelectricity; Solid State Physics Section, Atomic Physics Division. Author: 4.4
Tighe, Nancy J.: Defect studies by electron microscopy of non-metallic crystals; Physical Properties Section, Inorganic Solids Division. Author: 3.4
Torgesen, John L.: Ph.D. Columbia University, 1942; crystal growth from solutions, impurity retentions, crystal properties; Crystal Chemistry Section, Inorganic Solids Division. Author: 2.8

Vacher, Herbert C.: X-ray diffraction; Metallurgy Division. Author: 2.1
Van Valkenburg, Alvin: High-pressure transitions; Crystallography Section, Inorganic Solids Division. Author: 5.14
Wachtman, John B., Jr.: Ph.D. University of Maryland, 1961; mechanical and electrical properties of crystals; Chief, Physical Properties Section, Inorganic Solids Division. Author: 3.6;3.7;4.1
Wagman, Donald D.: Thermochemistry and chemical thermodynamics; Chief, Thermochemistry Section, Physical Chemistry Division. Author: 3.20
Wagner, Timothy: Growth and evaporation of whiskers; Crystallization of Metals Section, Metallurgy Division. Author: 2.21
Wasilik, John H.: Ph.D. Catholic University, 1956; dielectric constant and losses, ultrasonics; Solid State Physics Section, Atomic Physics Division. Author: 4.6
Weeks, James J.: Measurements of dielectric properties of polymers, crystallization and melting of polymers; Dielectric Section, Electricity Division. Author: 2.12
Weir, Charles E.: Infrared spectroscopy and high-pressure physics; Crystallography Section, Inorganic Solids Division. Author: 5.6;5.16
Wiederhorn, Sheldon M.: Ph.D. University of Illinois, 1960; optical properties of high pressure, fracture of solids; Physical Properties Section, Inorganic Solids Division. Author: 4.2
Will, Richard S.: Electron-field emission; Electron Physics Section, Atomic Physics Division.
Yolken, Howard T.: Growth of oxide films; Corrosion Section, Metallurgy Division. Author: 3.5
Young, John D.: Crystal growth by electrodeposition; Electrolysis and Metal Deposition Section, Metallurgy Division. Author: 2.16
Young, Russell D.: Ph.D. Pennsylvania State University, 1959; surface physics, particularly with the field-emission microscope; Electron Physics Section, Atomic Physics Division. Author: 2.25

Participants at the Boulder Laboratories

Arp, Vincent D.: Ph.D. University of California, 1959; superconductivity; Cryogenic Properties of Solids Section, Cryogenic Engineering Laboratory. Author: 4.20
Bamberger, Edwin C.: Dielectric measurements; Radio and Microwave Materials Section, Radio Standards Physics Division. Author: 4.7
Bussey, Howard E.: Ph.D. University of Colorado, 1964; magnetism and ferrites; Radio and Microwave Materials Section. Author: 4.18
Cook, Alan R.: Physical instrumentation; Radio and Microwave Materials Section, Radio Standards Physics Division. Author: 4.14
Dalke, John L.: Characterization of materials at radio frequencies; Chief, Radio and Microwave Materials Section, Radio Standards Physics Division. Author: 4.7
Gruzensky, Paul M.: Ph.D. Oregon State College, 1959; physical chemistry and high-purity materials; Radio and Microwave Materials Section, Radio Standards Physics Division.
Guntner, Charles S.: Imperfections, flow and fracture, phase transformations; Properties of Materials Section, Cryogenics Engineering Laboratories.
Jefferson, Clinton F.: Ph.D. University of Michigan, 1959; solid solution for ferrimagnetic characteristics; Radio and Microwave Materials Section, Radio Standards Physics Division.
Mahler, Robert J.: Ph.D. University of Colorado, 1963; solid state physics; Radio and Microwave Materials Section, Radio Standards Physics Division. Author: 4.14
Matarrese, Lawrence M.: Ph.D. University of Chicago, 1954; solid state physics, EPR resonance spectroscopy related to solid state mechanisms; Radio and Microwave Materials Section, Radio Standards Physics Division. Author: 4.14
Peterson, Robert L.: Ph.D. Lehigh University, 1959; theoretical physics; Radio and Microwave Materials Section, Radio Standards Physics Division. Author: 4.14

Powell, Robert L.: Thermal and electrical conduction of metals at low-temperatures; Properties of Materials Section, Cryogenic Engineering Laboratory.
Reed, Richard P.: Imperfections, flow and fracture, phase transformations; Properties of Materials Section, Cryogenic Engineering Laboratory.
Risley, Alan S.: Magnetism and ferrites; Radio and Microwave Materials Section, Radio Standards Physics Division. Author: 4.18
Wells, Joseph S.: Ph.D. University of Colorado, 1964; microwave physics, solid state physics relating to ENDOR and NMR; Radio and Microwave Materials Section, Radio Standards Physics Division. Author: 4.14
Winder, Dale R.: Ph.D. Case Institute of Technology, 1957; solid state physics; Radio and Microwave Materials Section, Radio Standards Physics Division. Author: 2.20

7. LITERATURE REFERENCES

S. Abramowitz and H. P. Broida (1963): Vibration of Methane in Condensed Oxygen, Nitrogen, and Argon; J. Chem. Phys., 39, 2383.

A. Bienenstock and G. Burley (1963): Thermal Expansion of Silver Iodide; J. Phys. Chem. Solids, 24, 1271.

I. A. Black, L. H. Bolz, F. P. Brooks, F. A. Mauer, and H. S. Peiser (1958): A Liquid-Helium Cold Cell for the Use with an X-Ray Diffractometer; J. Res. Nat'l. Bur. Standards, 61, 367.

S. Block, J. Molin, and G. Piermarini (1963): X-Ray Study of a Cadmium Borate Glass; J. Am. Ceram. Soc., 46, (11), 557.

S. Block and A. Perloff (1963): The Direct Determination of the Crystal Structure of $NaB(OH)_4.2H_2O$; Acta Cryst., 16, 1233.

G. Burley (1963a): Polymorphism of Silver Iodide; Am. Mineral., 48, 1266.

G. Burley (1963b): Photolytic Behavior of Silver Iodide; J. Res. Nat'l. Bur. Standards, 67A, 301.

R. deWit (1963): On the Growth of Helical Dislocations; Trans. AIME, 227, 1443.

R. K. Eby (1963): First Order Transition Temperature in Crystalline Polymers; J. Appl. Phys., 34, 2442.

R. K. Eby (1964): An Example of a Lamellar Copolymer; J. Res. Nat'l. Bur. Standards, 68A, (3).

R. A. Forman (1963): Nitrogen NMR Chemical Shifts in the Azide Ion; J. Chem. Phys., 39, 2393.

R. A. Forman and D. R. Like, Jr. (1963): Quadrupole Coupling Constants from the Microwave Spectrum of Hydrazoic Acid; J. Chem. Phys., 39, 1133.

A. D. Franklin (1963): Relaxation Modes for Trapped Crystal Point Defects; J. Res. Nat'l. Bur. Standards, 67A, 291.

A. D. Franklin, A. Shorb, and J. B. Wachtman, Jr. (1964): Relaxation Modes of Trapped Crystal Point Defects; a lecture to Brit. Ceram. Soc., Oct., 1963; for future publication in Trans. Brit. Ceram. Soc.

H. P. R. Frederikse, W. R. Thurber, and W. R. Hosler: Electronic Transport in Strontium Titanate; Phys. Rev., (accepted).

W. C. Hernandez, Jr. and A. H. Kahn (1963): A Note on the Galvanomagnetic and Thermoelectric Coefficients of Tetragonal Crystalline Materials; J. Res. Nat'l Bur. Standards, 67A, 293.

R. P. Hudson and B. W. Mangum (1963): Audio Frequency Dispersion Effects in Lanthanide Salts at Low Temperatures, in Magnetic and Electric Resonance and Relaxation; Wiley & Sons, Inc., J. Smidt, Tech. Univ. Delft, the Netherlands.

E. M. Levin and R. S. Roth (1964): Polymorphism of Bismuth Sesquioxide - I. Pure Bi_2O_3. II. Effect of Oxide Additions on the Polymorphism of Bi_2O_3; J. Res. Nat'l. Bur. Standards, 68A, (2).

F. A. Mauer and L. H. Bolz (1955): Measurement of Thermal Expansion of Cermet Components by High-Temperature X-Ray Diffraction; W A D C Technical Report, 55-474, 18.

F. Ogburn and C. Newton (1963): Relation of Partial (110) Pole Figures to Thickness and Microstructure of Electrodeposited Copper; J. Electrochem. Soc., 110 1148.

F. Ogburn, B. Paretzkin, and H. S. Peiser (1964): Pseudopentagonal Twins in Electrodeposited Copper Dendrites; Acta Cryst., 17, (accepted).

R. L. Parker, R. L. Anderson, and S.C. Hardy (1963): Growth and Evaporation Kinetics and Surface Diffusion of K and Hg Crystal Whiskers; Appl. Phys. Lett., 3, 93.

R. L. Parker and A. Krinsky (1963): Electrical Resistance-Strain Characteristics of Thin Evaporated Metal Films; J. Appl. Phys., 34, 2700.

H. S. Peiser, J. B. Wachtman, Jr., and R. W. Dickson (1963): Reduction of Space Groups to Subgroups by Homogeneous Strain; J. Res. Nat'l. Bur. Standards, 67A, 395.

A Perloff (1964): The Crystal Structure of 1-Ethyldecaborane; Acta Cryst., (accepted).

G. L. Pollack (1964): Absorption Spectra of Diatomic Molecules in Liquid and Crystalline Rare Gases; Advances in Applied Spectroscopy, Plenum Press, New York, (accepted).

F. A. Quinn, Jr. and J. Powers (1963): Measurements of a Maximum in the Isothermal Crystallization Rate Temperature Curve for Polypentene-1; J. Polymer Sci., Part B., 1, 341.

G. S. Ross and L. J. Frolen (1963): Chemical Purity by Dielectric Cryometry; J. Res. Nat'l. Bur. Standards, 67A, 607.

R. S. Roth and J. L. Waring (1963): Synthesis and Stability of Bismutotantalite, Stibotantalite, and Chemically Similar ABO_4 Compounds; Am. Mineral., 48, (11 & 12) 1348.

S. Ruthberg (1963): Thermal Behavior of Muscovite Sheet Mica; J. Res. Nat'l. Bur. Standards, 67A, 585.

S. Ruthberg, M. W. Barnes, and R. H. Noyce (1963): Correlation of Muscovite Sheet Mica on the Basis of Color, Apparent Optic Angle and Absorption Spectrum; J. Res. Nat'l. Bur. Standards, 67A, 309.

H. A. Schafft and J. C. French (1963): Second Breakdown; Effects of Base Drive and Structural Defects; a talk presented at the Electron Devices Meeting in Washington, D. C., Oct. 31, and printed as NBS Report No. 8122, Nov. 6.

S. J. Schneider (1963a): Compilation of the Melting Points of the Metal Ozides; Nat'l Bur. Standards Monograph, 68.

S. J. Schneider (1963b): Discrepancy in the Conversion of Early Melting Point Temperatures; J. Am. Ceram. Soc., 46, 354.

J. Simmons, R. W. Howard, and R. L. Parker (1964): Theory of Whisker Growth and Evaporation; J. Appl. Phys., (accepted).

J. Simmons R. L. Parker, and R. W. Howard (1964): Kinetics of Growth and Evaporation of Metal Whiskers; Bull. Am. Phys. Soc. (Philadelphia Meeting).

H. E. Swanson, E. H. Evans, and M. C. Morris (1964): Standard X-Ray Diffraction Powder Patterns; Nat'l. Bur. Standards Monograph, 25, Section 3.

L. J. Swartzendruber (1963): Four-Point Probe Measurement of Non-Uniformities in Semiconductor Sheet Resistivity; NBS Report No. 8066, Aug. 16. (To be published in more extensive form in NBS Tech. Note 199.)

N. J. Tighe (1964): Jet Thinning Device for Preparation of Al_2O_3 Electron Microscope Specimens; Rev. Sci. Instr., 35.

A. Van Valkenburg (1964): High-Pressure Microscopy of the Silver and Cuprous Halides; J. Res. Nat'l. Bur. Standards, 68A, 97.

J. B. Wachtman, Jr. (1963): Mechanical and Electrical Relaxation in ThO_2 Containing CaO; Phys. Rev., 131, 517.

J. B. Wachtman, Jr. and L. R. Doyle (1964): Internal Friction in Rutile Containing Point Defects; submitted to Phys. Rev.

J. B. Wachtman, Jr., M. L. Wheat, H. J. Anderson, and J. L. Bates (1964): Elastic Constants of Single Crystal UO_2 at 25°C; Submitted to J. Nuclear Materials.

J. Waring and R. S. Roth (1964): $10Me_2O_5.90Me_2O_5$ Tetragonal Phases Apparently Isostructural with $Ta_2O_5.2Nb_2O_5$; Acta Cryst. (accepted).

J. J. Weeks (1963): Melting Temperature and Change of the Lamellar Thickness with Time for Bulk Polyethylene; J. Res. Nat'l. Bur. Standards, 67A, 441.

C. E. Weir and G. J. Piermarini (1964a): Lattice Parameters and Lattice Energies of High-Pressure Polymorphs of Some Aldali Halides; J. Res. Nat'l. Bur. Standards, 68A, 105.

C. E. Weir and G. J. Piermarini (1964b): Allotropy in Some Rare-Earth Metals at High Pressures; Science (USA) (accepted).

R. S. Williams and G. L. Pollack (1964): Crystal Growth and Etching of Methane; Bull. Am. Phys. Soc., 9.

* U.S. GOVERNMENT PRINTING OFFICE : 1964 O—725-531